

OPTIMAL CONTROL STRATEGY TO CONTROL PANDEMIC COVID-19 USING $MSI_L I_H R_V$ MODEL

SHAHRIAR SEDDIGHI CHAHARBORJ¹, JALAL HASSANZADEH ASL^{1,*}
AND BABAK MOHAMMADI²

Abstract. Many researchers began doing studies about pandemic COVID-19 which began to spread from Wuhan, China in 2019 to all around the world and so far, numerous researches have been done around the world to control this contagious disease. In this paper, we proposed a $MSI_L I_H R_V$ mathematical model to study the spreading of pandemic COVID-19. This paper is aimed to study the vaccination effect in the control of the disease propagation rate. Another goal of this paper is to find the maximum number of susceptible people, minimum number of infected people, and the best value for number of vaccination people. The Jacobian matrix was obtained in the virus absenteeism equilibrium point for the proposed dynamical system. The spectral radius method was applied to find the analytical formula for the reproductive number. Reproductive number is one of the most benefit and important tools to study of epidemic model's stability and instability. In the following, by adding a controller to the model and also using the optimal control strategy, model performance was improved. To validate of the proposed models with controller and without controller we use the real data of COVID-19 from 4 January, 2021 up to 14 June, 2021 in Iran. Maple and MATLAB software's will be used for programming. We will use Maple software for analytical parts and MATLAB software for numerical and simulation parts.

Mathematics Subject Classification. 00A71, 34A34, 49-11, 49K15.

Received August 4, 2021. Accepted April 4, 2022.

1. INTRODUCTION

In this section, brief description of the infectious disease COVID-19 has been given, and we also explain mathematical modeling's and their applications in the modelling and analysis of infectious diseases.

1.1. Epidemic disease

In the 1960s, effectivity of vaccination programs, antibiotics and better sanitation established this certainty that infectious diseases would be eradicated soon; As a consequence, some chronic diseases like cardiovascular

Keywords and phrases: Pandemic disease, COVID-19, mathematical modelling, vaccination, equilibrium points, Jacobian matrix, reproductive number, control theory strategy, real data, validation.

¹ Department of Mathematics, Faculty of Science, Tabriz Branch, Islamic Azad University, Tabriz, Iran.

² Department of Mathematics, Marand Branch, Islamic Azad University, Marand, Iran.

* Corresponding author: jalal.hasanzadeh172@gmail.com

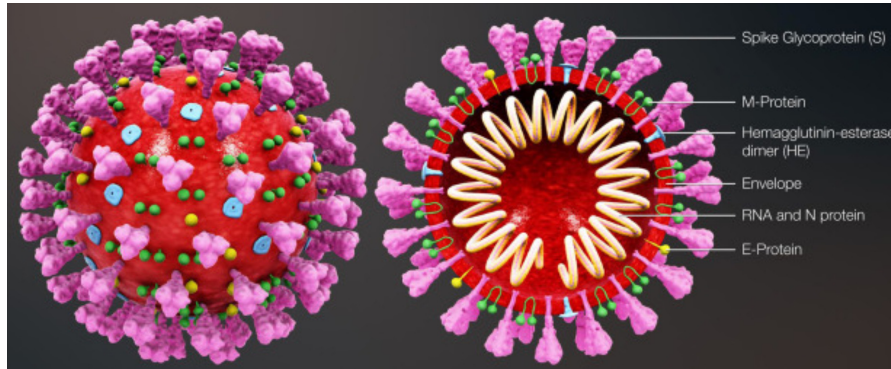


FIGURE 1. Structure of respiratory syndrome causing human coronavirus.

disease and cancer drew further attention in the industrialized countries and also in the United States; nevertheless, in the developing countries the infectious diseases remained as the chief reason behind mortality and suffer. Agents of the infectious diseases usually adjust and develop; however, new diseases have come forth, and some were already in existence, while some other diseases that had faded away, have re-appeared. Some examples on recently identified infectious diseases encircle hanta virus (1993), hepatitis E (1990), hepatitis C (1989), toxic-shock syndrome (1978), Legionnaire's disease (1976) and Lyme disease (1975); Moreover, the year 1981 faced the condition of human immunodeficiency virus (HIV). Then, Breeds of gonorrhoea, tuberculosis, and pneumonia that are resistant to antibiotics have developed [26, 30].

The coronavirus disease 2019 (COVID-19) pandemic is an ongoing crisis caused by severe acute respiratory syndrome coronavirus 2 (SARS-CoV-2). The *Nidovirales* order includes *Coronaviridae*, *Roniviridae*, and *Arteriviridae* families. One of the families of *Coronaviridae* is called coronavirus that is 65–125 nm in diameter and comprises a single-stranded RNA as a nucleic material. COVID-19 is a family of RNA Beta virus with a confined length of 26–32 kbs (Fig. 1) [38] in Nidoviral order. The first outbreak was detected in December 2019 in Wuhan, the capital of Hubei province, rapidly followed by the rest of Hubei and all other provinces in China. Within mainland China the epidemic was largely controlled by mid- to late March 2020, having generated >81,000 cases [12, 34, 43, 44].

Coronavirus disease 2019 (COVID-19) pandemic has imposed an unprecedented challenge to global health-care systems, societies, and governments [15, 47]. As of May 16, 2020, the severe acute respiratory syndrome coronavirus-2 (SARS-CoV-2, causative pathogen for COVID-19) has been detected in every country, with more than 4.6 million confirmed cases and a death toll exceeding 300,000 worldwide [15, 47, 49]. Furthermore, recent pandemic model projections estimate that COVID-19 could result in ~40 million deaths globally this year, if no interventions are implemented [15, 42, 47, 49]. Countries in Europe adopted different strategies to progressively phase out the strict restrictions put in place to curb COVID-19 pandemic [20, 21, 24, 25, 27]. They aimed to strike a delicate balance between reviving the economy and relieving social pressure while averting a potential resurgence of infections. Recent analyses suggest that various countries experienced disruptions to routine immunisation programmes or corresponding decreases in vaccine coverage, or both, in 2020, especially during the earlier phases of the COVID-19 pandemic [4, 7, 29, 31, 32, 45, 46, 48].

According to a poll of 260 health-care practitioners in May, 2020, respondents in 53 (85%) of 61 countries reported lower vaccination levels than those recorded in January and February, 2020 [48]. A systematic review of 17 observational studies found consistent declines in vaccine coverage and administered doses across locations and over time [29]. Additionally, the twenty-eighth meeting of the Emergency Committee under the International Health Regulations noted that ongoing COVID-19 transmission continues to pose a risk to polio eradication efforts, both for wild-type polio eradication activities and control of circulating vaccine-derived polioviruses [46]. Analyses across 21 countries in Europe, sub-Saharan Africa, north Africa and the Middle East,

and south Asia during the first half of 2020 found disruptions to childhood vaccination programmes of up to 90% [8, 31, 46].

1.2. Mathematical modelling

The mathematical modelling is a significant instrument/tool that enables the analysis and control of the infectious diseases outspread in a community. These models usually comprise of the parameters and different variables of a particular problem. The process of formulating a model clarifies the parameters, variables, and assumptions; likewise, these models render conceptual outputs like essential reproduction numbers, thresholds, and contact numbers. Both computer simulations and mathematical models are considered as valuable experimental tools proper for making and examining theories, answering particular related questions, evaluating quantitative hypotheses, specifying sensitivity to change the values of the related parameters, and to assess principal parameters from the input and output data.

Understanding the characteristics of infectious diseases transmissions in regions, countries, and communities might result in the development of better methods effective in reducing diseases transmissions. The mathematical models are usually used to plan, implement, compare, evaluate, and modify numerous programs of detection, treatment, control, and prevention of infectious diseases. As shown in Figure 2, chambers labelled M, S, E, I, and R, are usually used to denote epidemiological categories/groups. For instance, the category M hosts infants exhibiting negative immunity. Upon the disappearance of the maternal antibodies from bodies with passive immunity, the infant is transferred to class S which denotes susceptible individuals [5, 5, 6, 9, 10, 18, 36, 41].

Infants having no passive immunity, for the reason that their mothers have never developed infection, are allocated to the same class S, *i.e.*, of the individuals who might get infected. In case when there is enough contact between susceptible and infective individuals such that transmission takes place, then the susceptible individual is moved to class E which refers to the exposed individuals in the latent periods, that is, the infected individuals who are not seriously infectious. When the latency periods terminate, the person enters the infective individuals class I. This class corresponds to those individuals who are infectious, *i.e.* people who can transmit the infection. Upon the end of the infectious period, the formerly infectious individual joins class R which is made up of individuals having permanent infection, that is gained/developed immunity.

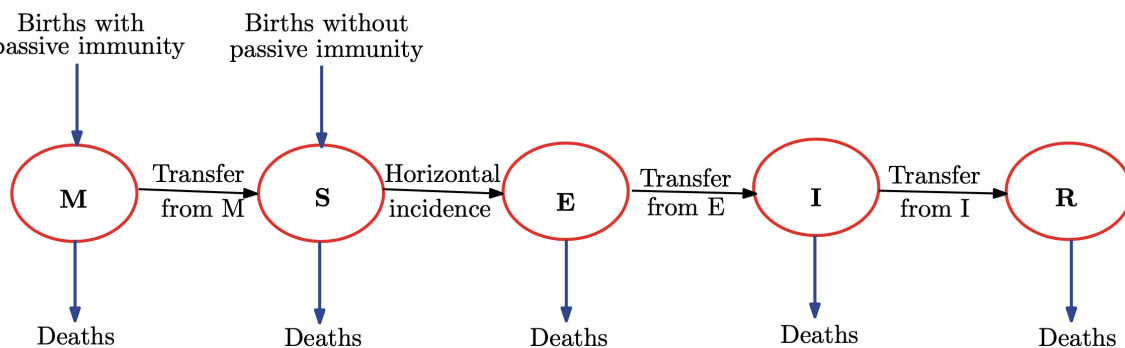
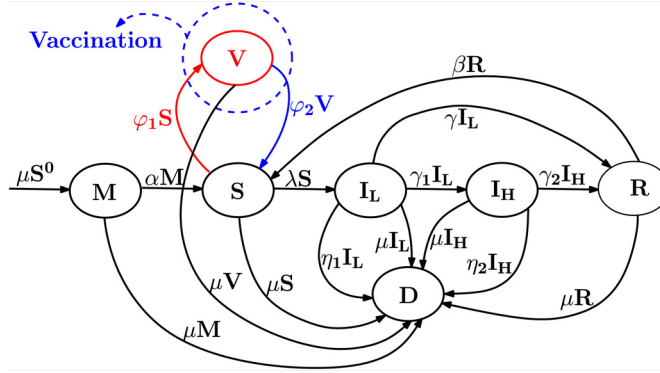


FIGURE 2. The general transfer diagram for epidemic disease model.

2. $MSI_L I_H R_V$ EPIDEMIC MODEL FOR COVID-19

Finding wrecking parameters involved in the propagation of COVID-19, detection strategies to stabilize coronavirus attacks, and prohibiting these attacks in the social network, are very significant. The presented

FIGURE 3. $MSI_L I_H R_V$ epidemic model for COVID-19.

model to study the COVID-19, as shown in Figure 3, includes five classes, class M shows healthy people who are resistant to the infection caused by coronavirus with congenital immunity, class S indicates the potentially susceptible (healthy) people in the social networks, I_L shows people who are completely infected by coronavirus, yet with less severity of infection, I_H shows people infected by coronavirus with high severity infection, class V indicated the vaccinated individuals (that is, that healthy people who already vaccinated prior to being attacked by coronavirus), people who are recovered from infection is shown by class R and class D shows the dead people. As shown in Figure 3, any of the determined classe has inputs and outputs.

In the social network, the newborns are entered into class M as constant migration μS_0 . Coefficient μ indicates the death rate of people for the the natural reasons; parameter α shows the transformation rate of healthy people with congenital immunity into healthy people without congenital immunity, parameters η_1 and η_2 show the death rates caused for the reason of the disease for classes I_L and I_H , respectively. The rate of recovered people from high severity infection individuals is shown by parameter γ_2 . The rate of recovered people from infection with less and high severity infection are defined with the parameters γ and γ_2 , respectively. The rate of vaccinated individuals from among susceptible people is shown by parameter φ_1 , parameter φ_2 indicates the transformation rate of vaccinated individuals into susceptible individuals and increase of susceptible people from the recovered people can be defined with rate β . The infection rate, $\lambda = cpI_L/N$, depends on the transmission probability per partner ($p > 0$), number of partners per individual per unit time ($c > 0$) and the ratio of infected individuals to infection active individuals I_L/N , with $N = M + S + I_L + I_H + R + V$ (N is total population size). In the following, the transmission dynamic system of $MSI_L I_H R_V$ model for the pandemic COVID-19 can be defined as follows [18],

$$\begin{cases} \frac{dM}{dt} = \mu S^0 - \alpha M - \mu M, \\ \frac{dS}{dt} = \alpha M + \varphi_2 V + \beta R - \mu S - \varphi_1 S - \lambda S, \\ \frac{dI_L}{dt} = \lambda S - \mu I_L - \eta_1 I_L - \gamma I_L - \gamma_1 I_L, \\ \frac{dI_H}{dt} = \gamma_1 I_L - \mu I_H - \eta_2 I_H - \gamma_2 I_H, \\ \frac{dR}{dt} = \gamma I_L + \gamma_2 I_H - \mu R - \beta R, \\ \frac{dV}{dt} = \varphi_1 S - \varphi_2 V, \\ \frac{dD}{dt} = \mu (M + S + I_L + I_H + R + V) + \eta_1 I_L + \eta_2 I_H, \end{cases} \quad (2.1)$$

with initial conditions $M(0) = M_0$, $S(0) = S_0$, $I_L(0) = I_{L,0}$, $I_H(0) = I_{H,0}$, $R(0) = R_0$ and $D(0) = D_0$; where, $\lambda = cpI/N$ and $N = M + S + V + I_L + I_H + R$. The conceivable region for the proposed system (2.1) can be defined as follows,

$$\Omega = \left\{ (M, S, I_L, I_H, R, V) \left| M + S + I_L + I_H + R + V \leq \frac{\mu S^0}{\alpha + \mu}, M > 0, S > 0, I_L > 0, I_H > 0, R > 0, V > 0 \right. \right\}.$$

2.1. Trivial, virus absenteeism and incidence equilibriums

Trivial equilibrium (TE) for the system (2.1) is as follows,

$$\text{TE : } (M, S, V, I_L, I_H, R) = (0, 0, 0, 0, 0, 0),$$

virus absenteeism equilibrium (VAE) can be defined as follows,

$$\text{VAE : } (M^0, S^0, V^0, I_L^0, I_H^0, R^0) = \left(\frac{\mu S^0}{\alpha + \mu}, \frac{\alpha S^0}{\alpha + \mu}, \frac{\alpha \varphi_1 S^0}{\varphi_2 (\alpha + \mu)}, 0, 0, 0 \right),$$

and virus incidence equilibrium (VIE) is defined as follows,

$$\text{VIE : } (S^*, I_L^*, I_H^*, R^*, Q^*) = (\mathcal{M}, \mathcal{S}, \mathcal{V}, \mathcal{I}_L, \mathcal{I}_H, \mathcal{R});$$

$$\mathcal{M} = \frac{\mu S^0}{\alpha + \mu},$$

$$\begin{aligned} \mathcal{S} = & \Upsilon_1 \left[(\mu^4 \varphi_1 + (\eta_1 (2\varphi_1 + \varphi_2) + \beta \varphi_1 + (2\gamma + \eta_2 + 2\gamma_1 + \gamma_2) \varphi_1 - \varphi_2 cp) \mu^3 \right. \\ & + (\eta_1^2 (\varphi_1 + \varphi_2) \\ & + (\beta (2\varphi_1 + \varphi_2) + (2\gamma + 2\eta_2 + 2\gamma_1 + 2\gamma_2) \varphi_1 + \varphi_2 (\gamma + \gamma_1 + \gamma_2 + \eta_2 - cp)) \eta_1 \\ & + ((\gamma + 2\gamma_1 + \gamma_2 + 2\eta_2) \varphi_1 - \varphi_2 cp) \beta + (\gamma + \gamma_1) (\gamma + 2\eta_2 + \gamma_1 + 2\gamma_2) \varphi_1 \\ & - \varphi_2 ((cp - \gamma_1) \eta_2 + cp (\gamma + \gamma_1 + \gamma_2))) \mu^2 \\ & + ((\varphi_1 + \varphi_2) (\beta + \eta_2 + \gamma_2) \eta_1^2 \\ & + (((\gamma + 2\eta_2 + 2\gamma_1 + 2\gamma_2) \varphi_1 + \varphi_2 (\gamma + \eta_2 + \gamma_1 + \gamma_2 - cp)) \beta \\ & + 2 (\eta_2 + \gamma_2) (\gamma + \gamma_1) \varphi_1 + \varphi_2 ((\gamma + 2\gamma_1 - cp) \eta_2 + \gamma_2 (\gamma + \gamma_1 - cp))) \eta_1 \\ & + (((\gamma + 2\gamma_1) \eta_2 + (\gamma_1 + \gamma_2) (\gamma + \gamma_1)) \varphi_1 + ((\gamma_1 - cp) \eta_2 - cp (\gamma_1 + \gamma_2)) \varphi_2) \beta \\ & + ((\eta_2 + \gamma_2) (\gamma + \gamma_1) \varphi_1 + \varphi_2 ((\gamma_1 - cp) \eta_2 - \gamma_2 cp)) (\gamma + \gamma_1)) \mu \\ & \left. + \beta ((\eta_2 + \gamma_2) \eta_1 + \eta_2 \gamma_1) ((\varphi_1 + \varphi_2) \eta_1 + (\gamma + \gamma_1) \varphi_1 + \varphi_2 (\gamma + \gamma_1 - cp)) \right] (\alpha \\ & + \mu)^{-1}, \end{aligned}$$

$$\begin{aligned} \mathcal{V} = & \Upsilon_2 \left[(\alpha + \mu) (\mu^4 \varphi_1 + ((2\varphi_1 + \varphi_2) \eta_1 + \beta \varphi_1 + (2\gamma + 2\gamma_1 + \gamma_2 + \eta_2) \varphi_1 - \varphi_2 cp) \mu^3 \right. \\ & + ((\varphi_1 + \varphi_2) \eta_1^2 + ((2\varphi_1 + \varphi_2) \beta) + (2\gamma + 2\gamma_1 + 2\gamma_2 + 2\eta_2) \varphi_1 \\ & + \varphi_2 (\gamma + \gamma_1 + \gamma_2 + \eta_2 - cp)) \eta_1 \\ & + (((\gamma + 2\gamma_1 + \gamma_2 + \eta_2) \varphi_1 - \varphi_2 cp) \beta + (\gamma + \gamma_1) (\gamma + \gamma_1 + 2\gamma_2 + 2\eta_2) \varphi_1 \\ & - ((cp - \gamma_1) \eta_2 + cp (\gamma + \gamma_1 + \gamma_2)) \varphi_2) \mu^2 + ((\varphi_1 + \varphi_2) (\beta + \gamma_2 + \eta_2) \eta_1^2 \\ & + (((\gamma + 2\gamma_1 + 2\gamma_2 + 2\eta_2) \varphi_1 + \varphi_2 (\gamma + \gamma_1 + \gamma_2 + \eta_2 - cp)) \beta \\ & \left. + 2 (\gamma_2 + \eta_2) (\gamma_1 + \gamma_2) \varphi_1 + ((\gamma + 2\gamma_1 - cp) \eta_2 + \gamma_2 (\gamma + \gamma_1 - cp)) \varphi_2) \eta_1 \right] \end{aligned}$$

$$\begin{aligned}
& + (((\gamma + 2\gamma_1)\eta_2 + (\gamma + \gamma_1)(\gamma_1 + \gamma_2))\varphi_1 + \varphi_2((\gamma_1 - cp)\eta_2 - cp(\gamma_1 + \gamma_2)))\beta \\
& + ((\gamma_2 + \eta_2)(\gamma + \gamma_1)\varphi_1 + ((\gamma_1 - cp)\eta_2 - \gamma_2 cp)\varphi_2)(\gamma + \gamma_1)\mu \\
& + ((\gamma_2 + \eta_2)\eta_1 + \eta_2\gamma_1)\beta((\varphi_1 + \varphi_2)\eta_1 + (\gamma_1 + \gamma_2)\varphi_1 + \varphi_2(\gamma + \gamma_1 - cp))^{-1},
\end{aligned}$$

$$\begin{aligned}
\mathcal{I}_L = \Upsilon_3 & [(\alpha + \mu)(\mu^4\varphi_1 + ((\beta + 2\gamma + 2\eta_1 + \eta_2 + 2\gamma_1 + \gamma_2)\varphi_1 + \varphi_2(\eta_1 - cp))\mu^3 \\
& + ((\eta_1^2 + (2\beta + 2\gamma + 2\gamma_1 + 2\gamma_2 + 2\eta_2)\eta_1 + (\gamma + 2\gamma_1 + \gamma_2 + \eta_2)\beta) \\
& + (\gamma + \gamma_1)(\gamma + \gamma_1 + 2\gamma_2 + 2\eta_2)\varphi_1 \\
& + (\eta_1^2 + (\beta + \gamma + \gamma_1 + \gamma_2 + \eta_2 - cp)\eta_1 - \beta cp + (\eta_2 - cp)\gamma_1 \\
& - cp(\gamma_1 + \gamma_2 + \eta_2))\varphi_2)\mu^2 \\
& + (((\beta + \gamma_2 + \eta_2)\eta_1^2 + ((\gamma + 2\gamma_1 + 2\gamma_2 + 2\eta_2)\beta) + 2(\gamma_2 + \eta_2)(\gamma + \gamma_1))\eta_1 \\
& + (\gamma_1^2 + (\gamma + \gamma_2 + 2\eta_2)\gamma_1 + \gamma(\gamma_2 + \eta_2))\beta + (\gamma + \gamma_1)^2(\gamma_2 + \eta_2))\varphi_1 \\
& + ((\beta + \gamma_2 + \eta_2)\eta_1^2 \\
& + ((\gamma + \gamma_1 + \gamma_2 + \eta_2 - cp)\beta + (\gamma_2 + 2\eta_2)\gamma_1 + (\gamma_2 + \eta_2)(\gamma - cp)\eta_1 \\
& + ((\eta_2 - cp)\gamma_1 - cp(\gamma_2 + \eta_2))\beta + (\gamma_1\eta_2 - cp(\gamma_2 + \eta_2))(\gamma + \gamma_1))\varphi_2)\mu \\
& + \beta((\gamma_2 + \eta_2)\eta_1 + \gamma_1\eta_2)((\gamma + \gamma_1 + \eta_1)\varphi_1 + \varphi_2(\gamma + \gamma_1 + \eta_1 - cp))^{-1},
\end{aligned}$$

$$\begin{aligned}
\mathcal{I}_H = \gamma\mu S^0(\mu + \beta) & [((\varphi_1 + \varphi_2)\mu + (\gamma + \gamma_1 + \eta_1)\varphi_1 + \varphi_2(\gamma + \gamma_1 + \eta_1 - cp))\alpha \\
& + \varphi_2\mu(\gamma + \gamma_1 + \eta_1 + \mu)]\mathcal{I}_L,
\end{aligned}$$

$$\begin{aligned}
\mathcal{R} = \mu S^0(\mu\gamma + \gamma_1\gamma_2 \\
& + \gamma(\gamma_2 + \eta_2)) [((\varphi_1 + \varphi_2)\mu + (\gamma + \gamma_1 + \eta_1)\varphi_1 + \varphi_2(\gamma + \gamma_1 + \eta_1 - cp))\alpha \\
& + \varphi_2\mu(\gamma + \gamma_1 + \eta_1 + \mu)]\mathcal{I}_L,
\end{aligned}$$

where, Υ_1 , Υ_2 and Υ_3 are defined as follows,

$$\begin{aligned}
\Upsilon_1 = -\mu\varphi_2 S^0(\mu + \gamma + \gamma_1 \\
& + \eta_1)((\mu^2 + (\beta + \gamma + \gamma_1 + \gamma_2 + \eta_2)\mu + (\gamma_1 + \gamma_2 + \eta_2)\beta + \gamma\eta_2 \\
& + \gamma_2(\gamma_1 + \gamma_2))\alpha + \mu^3 + (\beta + \gamma_1 + \gamma_2 + \eta_1 + \eta_2)\mu^2 \\
& + ((\beta + \gamma_2 + \eta_2)\eta_1 + (\gamma_1 + \gamma_2 + \eta_2)\beta + (\gamma_2 + \eta_2)(\gamma + \gamma_1))\mu \\
& + \beta((\gamma_2 + \eta_2)\eta_1 + \eta_2\gamma_1)),
\end{aligned}$$

$$\begin{aligned}
\Upsilon_2 = -\mu\varphi_1 S^0(\mu + \gamma + \gamma_1 \\
& + \eta_1)((\mu^2 + (\beta + \gamma + \gamma_1 + \gamma_2 + \eta_2)\mu + (\gamma_1 + \gamma_2 + \eta_2)\beta + \gamma\eta_2 \\
& + \gamma_2(\gamma_1 + \gamma_2))\alpha + \mu^3 + (\beta + \gamma + \gamma_1 + \gamma_2 + \eta_1 + \eta_2)\mu^2 \\
& + ((\beta + \gamma_2 + \eta_2)\eta_1 + (\gamma_1 + \gamma_2 + \eta_2)\beta + (\gamma_2 + \eta_2)(\gamma + \gamma_1))\mu \\
& + ((\gamma_2 + \eta_2)\eta_1 + \eta_2\gamma_1)\beta),
\end{aligned}$$

$$\begin{aligned}
\Upsilon_3 = \mu S^0(\mu + \beta)(\mu + \gamma_2 + \eta_2) & [((\varphi_1 + \varphi_2)\mu + (\gamma + \gamma_1 + \eta_1)\varphi_1 + \varphi_2(\gamma + \gamma_1 + \eta_1 - cp))\alpha \\
& + \varphi_2\mu(\gamma + \gamma_1 + \eta_1 + \mu)].
\end{aligned}$$

2.2. Linearizing of the proposed system for $MSI_L I_H R_V$ model

Linearized of system (2.1) around the virus absenteeism equilibrium is given by,

$$\begin{cases} \frac{dM}{dt} = \mu S^0 - \alpha M - \mu M, \\ \frac{dS}{dt} = \alpha M + \varphi_2 sV + \beta R - \mu S - \varphi_1 S - cpI_L \\ \frac{dI_L}{dt} = cpI_L - \mu I_L - \eta_1 I_L - \gamma I_L - \gamma_1 I_L, \\ \frac{dI_H}{dt} = \gamma_1 I_L - \mu I_H - \eta_2 I_H - \gamma_2 I_H, \\ \frac{dR}{dt} = \gamma I_L + \gamma_2 I_H - \mu R - \beta R, \\ \frac{dV}{dt} = \varphi_1 S - \varphi_2 V, \\ \frac{dD}{dt} = \eta(M + S + I_L + I_H + R + V) + \eta_1 I_L + \gamma_2 I_H, \end{cases} \quad (2.2)$$

Hence, can derive the Jacobian matrix for the linearized system (2.2) around the virus absenteeism equilibrium as follows,

$$J(\text{VAE}) = \begin{bmatrix} \frac{\partial F_1}{\partial M} & \frac{\partial F_1}{\partial S} & \frac{\partial F_1}{\partial V} & \frac{\partial F_1}{\partial I_L} & \frac{\partial F_1}{\partial I_H} & \frac{\partial F_1}{\partial R} \\ -\alpha - \mu & 0 & 0 & 0 & 0 & 0 \\ 0 & -\mu - \varphi_1 & \varphi_2 & -cp & 0 & \beta \\ 0 & 0 & 0 & cp - \mathcal{K} & 0 & 0 \\ 0 & 0 & 0 & \gamma_1 & -\mu - \gamma_2 - \eta_2 & 0 \\ 0 & 0 & 0 & \gamma & \gamma_2 & -\mu - \beta \\ 0 & \varphi_1 & -\varphi_2 & 0 & 0 & 0 \end{bmatrix} \quad (2.3)$$

where, $\mathcal{K} = \mu + \gamma + \gamma_1 + \eta_1$ and $F_1 = \dot{M}$, $F_2 = \dot{S}$, $F_3 = \dot{V}$, $F_4 = \dot{I}_L$, $F_5 = \dot{I}_H$.

2.3. Reproductive number

The spectral radius of the next generation operator will help us to find an explicit formula for the reproductive number. According the Jacobian matrix (2.3), along with virus absenteeism equilibrium (VAE), the transmission matrix F and transition matrix V [1, 5, 10, 36, 41] can be defined as follows,

$$F = \begin{bmatrix} 0 & 0 & 0 & 0 & 0 & 0 \\ \alpha & 0 & \varphi_2 & 0 & 0 & \beta \\ 0 & 0 & 0 & cp & 0 & 0 \\ 0 & 0 & 0 & \gamma_1 & 0 & 0 \\ 0 & 0 & 0 & \gamma & \gamma_2 & 0 \\ 0 & \varphi_1 & 0 & 0 & 0 & 0 \end{bmatrix},$$

and

$$V = \begin{bmatrix} \alpha + \mu & 0 & 0 & 0 & 0 & 0 \\ \alpha & \mu + \varphi_1 & 0 & cp & 0 & \beta \\ 0 & 0 & 0 & \mu + \gamma + \gamma_1 + \eta_1 & 0 & 0 \\ 0 & 0 & 0 & 0 & \mu + \gamma_2 + \eta_2 & 0 \\ 0 & 0 & 0 & 0 & 0 & \mu + \beta \\ 0 & 0 & \varphi_2 & 0 & 0 & 0 \end{bmatrix},$$

where, F is a nonnegative matrix, V is a non-singular matrix and $J(\text{VAE}) = F - V$. Hence, the reproductive number, \mathcal{R}_0 , is equal to the spectral radius $\rho(FV^{-1})$ [11, 14, 19, 37, 41]. Matrix V^{-1} , invers of matrix V is giving by,

$$V^{-1} = \begin{bmatrix} \frac{1}{\alpha + \mu} & 0 & 0 & 0 & 0 & 0 & 0 \\ 0 & \frac{1}{\mu + \varphi_1} & 0 & -\frac{cp}{(\mu + \gamma + \gamma_1 + \eta_1)(\mu + \varphi_1)} & 0 & 0 & 0 \\ 0 & 0 & 0 & \frac{1}{\mu + \gamma + \gamma_1 + \eta_1} & 0 & 0 & 0 \\ 0 & 0 & 0 & 0 & \frac{1}{\mu + \gamma_2 + \eta_2} & 0 & 0 \\ 0 & 0 & 0 & 0 & 0 & \frac{1}{\mu + \beta} & 0 \\ 0 & 0 & \frac{1}{\varphi_2} & 0 & 0 & 0 & 0 \end{bmatrix}$$

therefore, the reproductive number \mathcal{R}_0 is deriving as follows,

$$\begin{aligned} \mathcal{R}_0 = \rho(FV^{-1}) &= \rho \left(\begin{bmatrix} 0 & 0 & 0 & 0 & 0 & 0 & 0 \\ \frac{\alpha}{\mu + \varphi_1} & 0 & \frac{\varphi_2}{\mu + \varphi_1} & -\frac{c^2 p^2}{(\mu + \gamma + \gamma_1 + \eta_1)(\mu + \varphi_1)} & 0 & \frac{\beta}{\mu + \varphi_1} & 0 \\ 0 & 0 & 0 & \frac{cp}{\mu + \gamma + \gamma_1 + \eta_1} & 0 & 0 & 0 \\ 0 & 0 & 0 & \frac{\gamma_1}{\mu + \gamma_2 + \eta_2} & 0 & 0 & 0 \\ 0 & 0 & 0 & \frac{\gamma}{\mu + \beta} & \frac{\gamma_2}{\mu + \beta} & 0 & 0 \\ 0 & \frac{\varphi_1}{\varphi_2} & 0 & 0 & 0 & 0 & 0 \end{bmatrix} \right) \\ &= \max \left\{ \frac{cp}{\mu + \gamma + \gamma_1 + \eta_1}, \sqrt{\frac{\varphi_1}{\mu + \varphi_1}} \right\} = \frac{cp}{\mu + \gamma + \gamma_1 + \eta_1}; \quad \left(\sqrt{\frac{\varphi_1}{\mu + \varphi_1}} < 1 \right), \end{aligned}$$

Theorem 2.1. *The proposed system (2.1) around VAE: $(\frac{\mu S^0}{\alpha + \mu}, \frac{\alpha S^0}{\alpha + \mu}, \frac{\alpha \varphi_1 S^0}{\varphi_2(\alpha + \mu)}, 0, 0, 0)$ is locally asymptotical stable if $\mathcal{R}_0 < 1$.*

Proof. Characteristic Polynomial (CP) for the Jacobian matrix can be derived as follows,

$$P(\lambda) = |J(\text{VAE}) - \mathcal{Y}I| = \begin{vmatrix} -\alpha - \mu - \mathcal{Y} & 0 & 0 & 0 & 0 & 0 \\ \alpha & -\mu - \varphi_1 - \mathcal{Y} & \varphi_2 & -cp & 0 & \beta \\ 0 & 0 & -\mathcal{Y} & cp - \mathcal{K} & 0 & 0 \\ 0 & 0 & 0 & \gamma_1 - \mathcal{Y} & -\mu - \gamma_2 - \eta_2 & 0 \\ 0 & 0 & 0 & \gamma & \gamma_2 - \mathcal{Y} & -\mu - \beta \\ 0 & \varphi_1 & -\varphi_2 & 0 & 0 & -\mathcal{Y} \end{vmatrix} \\ = 0,$$

with $\mathcal{K} = \mu + \gamma + \gamma_1 + \eta_1$. Therefore, the eigenvalues can be listed as follows,

$$\begin{aligned} \mathcal{Y}_1 &= -\frac{1}{2} \left(\mu + \varphi_1 + \varphi_2 - \sqrt{\mu^2 + 2\mu\varphi_1 - 2\mu\varphi_2 + 2\varphi_1\varphi_2 + \varphi_1^2 + \varphi_2^2} \right), \\ \mathcal{Y}_2 &= -\frac{1}{2} \left(\mu + \varphi_1 + \varphi_2 + \sqrt{\mu^2 + 2\mu\varphi_1 - 2\mu\varphi_2 + 2\varphi_1\varphi_2 + \varphi_1^2 + \varphi_2^2} \right), \end{aligned}$$

$$\mathcal{Y}_3 = -\mu - \eta_2 - \gamma_2, \quad \mathcal{Y}_4 = -\mu - \beta, \quad \mathcal{Y}_5 = -\mu - \alpha, \quad \mathcal{Y}_6 = cp - (\mu + \gamma + \gamma_1 + \eta_1),$$

It is clear that, the eigenvalues \mathcal{Y}_2 , \mathcal{Y}_3 , \mathcal{Y}_4 and \mathcal{Y}_5 are negative. Easily can show that the eigenvalue \mathcal{Y}_2 is negative also,

$$\begin{aligned} 2\mu\varphi_1 > -4\mu\varphi_2 &\implies 2\mu\varphi_1 + 2\mu\varphi_2 > -2\mu\varphi_2 \\ &\implies 2\mu\varphi_1 + 2\mu\varphi_2 + \varphi_1^2 + \varphi_2^2 + \mu^2 + 2\varphi_1\varphi_2 \\ &> -2\mu\varphi_2 + \varphi_1^2 + \varphi_2^2 + \mu^2 + 2\varphi_1\varphi_2 \\ &\implies (\mu + \varphi_1 + \varphi_2)^2 > \mu^2 + 2\mu\varphi_1 - 2\mu\varphi_2 + 2\varphi_1\varphi_2 + \varphi_1^2 + \varphi_2^2 \\ &\implies \mu + \varphi_1 + \varphi_2 > \sqrt{\mu^2 + 2\mu\varphi_1 - 2\mu\varphi_2 + 2\varphi_1\varphi_2 + \varphi_1^2 + \varphi_2^2} \end{aligned}$$

therefore, we have,

$$\mathcal{Y}_1 = -\frac{1}{2} \left(\mu + \varphi_1 + \varphi_2 - \sqrt{\mu^2 + 2\mu\varphi_1 - 2\mu\varphi_2 + 2\varphi_1\varphi_2 + \varphi_1^2 + \varphi_2^2} \right) < 0.$$

Now, the second order Routh-Hurwitz criterion is applied to derived passable eigenvalue (\mathcal{Y}_6),

$$cp - (\mu + \gamma + \gamma_1 + \eta_1) < 0, \quad cp < \mu + \gamma + \gamma_1 + \eta_1 \implies \mathcal{R}_0 = \frac{cp}{\mu + \gamma + \gamma_1 + \eta_1} < 1,$$

therefore, the virus absenteeism equilibrium given by Routh-Hurwitz criteria as follows,

$$(M^0, S^0, V^0, I_L^0, I_H^0, R^0) = \left(\frac{\mu S^0}{\alpha + \mu}, \frac{\alpha S^0}{\alpha + \mu}, \frac{\alpha \varphi_1 S^0}{\varphi_2 (\alpha + \mu)}, 0, 0, 0 \right),$$

is locally asymptotical stable. □

2.4. Study of sensitive parameters

The stability, instability and criticality of the proposed model depend on the parameters appearing in the reproductive number. Therefore, we study the sensitivity of the reproductive number, \mathcal{R}_0 , relative to the parameters $0 < \mu < 1$, $0 < \gamma < 1$, $0 < \gamma_1 < 1$, $0 < \eta_1 < 1$, $0 < p < 1$ and $c > 0$ in order to be equal to one ($\mathcal{R}_0 = 1$) or less than one ($\mathcal{R}_0 < 1$) or greater than one ($\mathcal{R}_0 > 1$). Figure 4 shows the stability and instability regions of transmission probability per partner *versus* the number of partners per individual per unit time when $\mu = 0.05$, $\gamma = 0.6$, $\gamma_1 = 0.08$, $\eta_1 = 0.03$. Stability and instability regions of death rate of people for the natural reasons *versus* the rate of recovered people from infection with less severity infection when $c = 4$, $p = 0.35$, $\gamma_1 = 0.08$, $\eta_1 = 0.03$ is indicated in the Figure 5. As can be seen from Figures 4 and 5, by increasing the parameter c for small values of the parameter p the stability region becomes smaller hurriedly, and for small values of the parameter c by increasing the parameter p also the stability region becomes small rapidly. Figure 5 shows that with increasing the parameters μ and γ at the same time, the stability region becomes larger. Figures 6–9 show the reproductive number of proposed model *vs.* μ and γ , μ and γ_1 , μ and η_1 , μ and γ_1 respectively when $c = 3$, $p = 0.35$, $\gamma = 0.6$, $\gamma_1 = 0.02$, $\eta_1 = 0.03$. Presented figure's, indicate the behaviors of pandemic COVID-19 for the modes of stability, criticality and instability of the proposed epidemic model dynamical system.

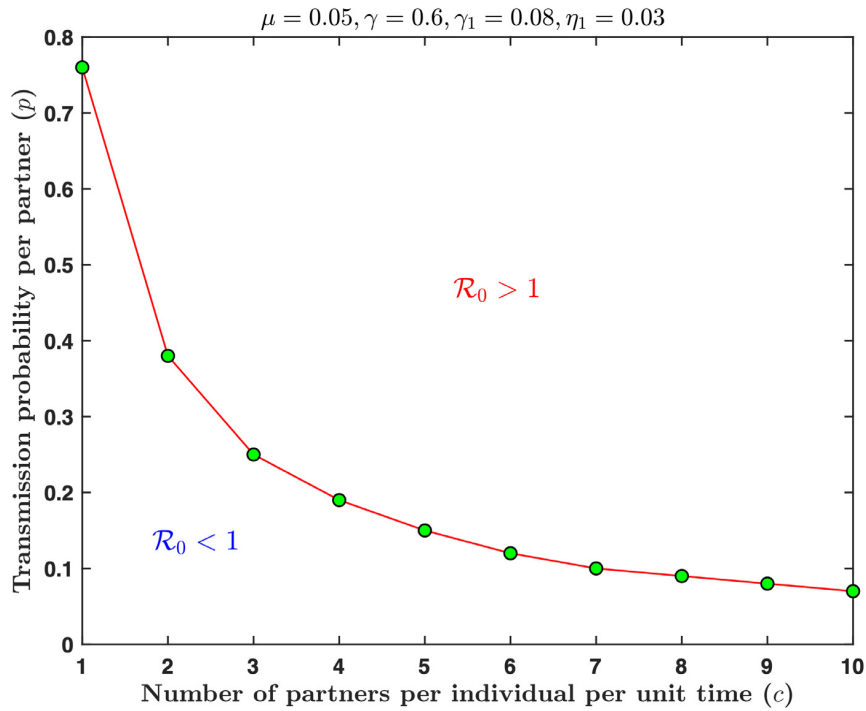


FIGURE 4. Stability and instability regions of c versus p when $\mu = 0.05$, $\gamma = 0.6$, $\gamma_1 = 0.08$, $\eta_1 = 0.03$.

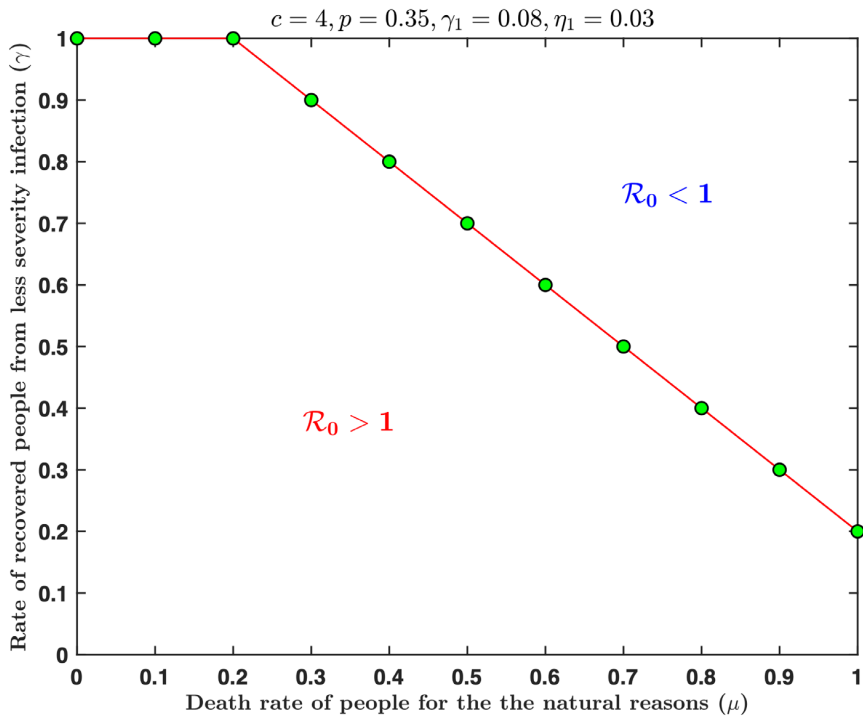


FIGURE 5. Stability and instability regions of μ versus γ when $c = 4$, $p = 0.35$, $\gamma_1 = 0.08$, $\eta_1 = 0.03$.

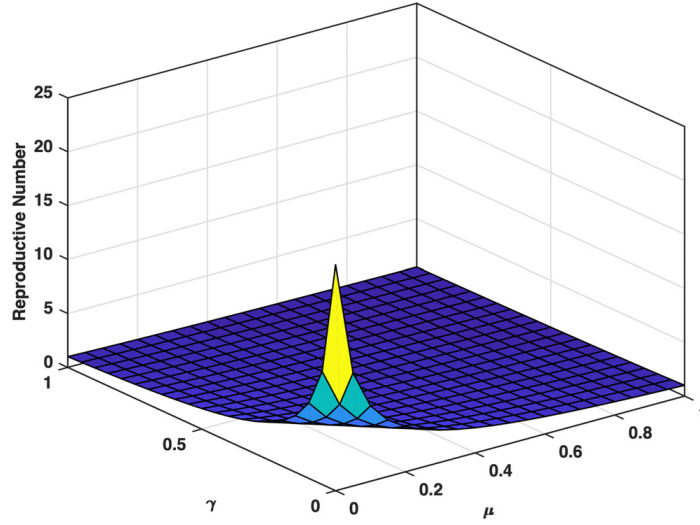


FIGURE 6. Reproductive number *vs.* μ and γ when $c = 4$, $p = 0.35$, $\gamma_1 = 0.08$, $\eta_1 = 0.03$.

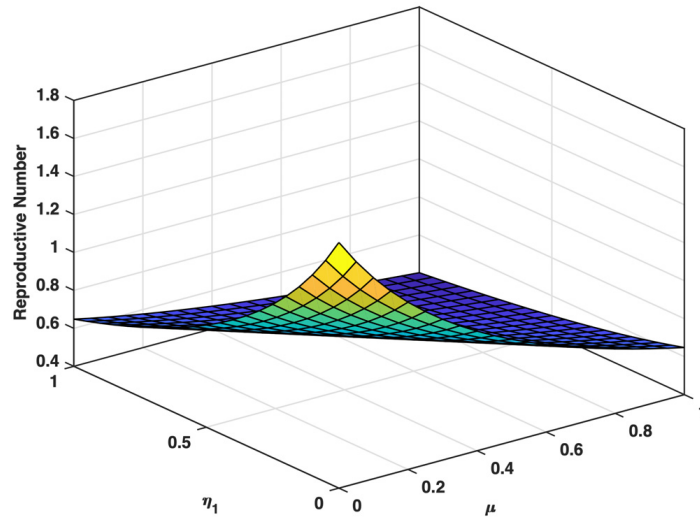


FIGURE 7. Reproductive number *vs.* μ and γ_1 when $c = 4$, $p = 0.35$, $\gamma = 0.6$, $\eta_1 = 0.03$.

2.5. Stability analysis

When there is a bifurcation at reproductive number equal to 1 ($\mathcal{R}_0 = 1$), the disease invade to population wouldn't be feasible if $\mathcal{R}_0 < 1$, because with entering some infected individuals into the population, the system would then return to the disease-free equilibrium $I_L = 0$. For values of reproductive number, whatever greater than 1 and E^0 is shifted from stability to instability; in this case, the model embraces a unique endemic equilibrium, which is locally asymptotically stable [28, 33]. To indicate the stability and existence of endemic equilibrium for the proposed model we find the contact rate of c , from reproductive equation as

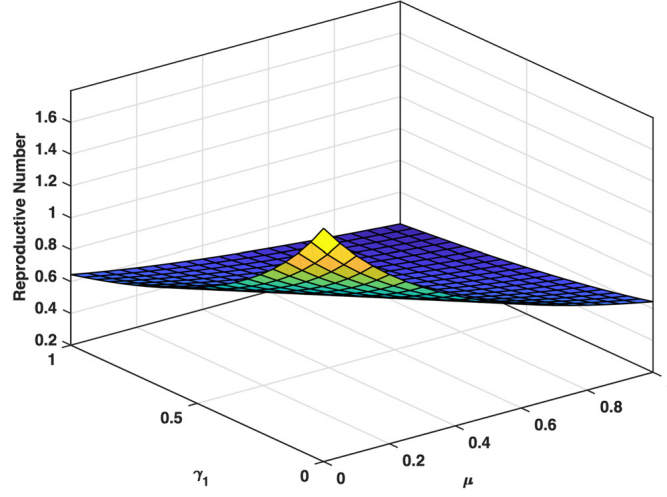


FIGURE 8. Reproductive number *vs.* μ and η_1 when $c = 4$, $p = 0.35$, $\gamma = 0.6$, $\gamma_1 = 0.08$.

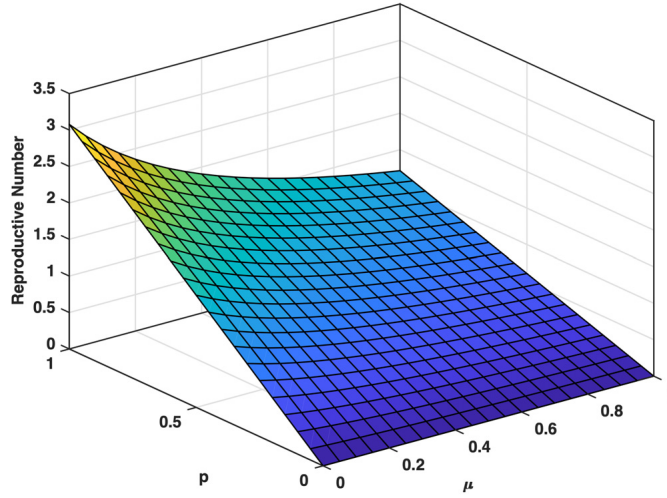


FIGURE 9. Reproductive number *vs.* μ and p when $c = 4$, $\gamma = 0.6$, $\gamma_1 = 0.08$, $\eta_1 = 0.03$.

follows,

$$c = \frac{\mathcal{R}_0}{p} (\mu + \gamma + \gamma_1 + \eta_1),$$

by placing this equation in the I_L^* we will have,

$$I_L^*(\mathcal{R}_0) = \mathcal{M} \times \left\{ ((\varphi_2 \mathcal{R}_0 - \varphi_1) \mu^3 + (((\gamma_1 + \gamma_2 + \gamma + \eta_1 + \eta_2 + \beta) \mathcal{R}_0 - \eta_1) \varphi_2 \right.$$

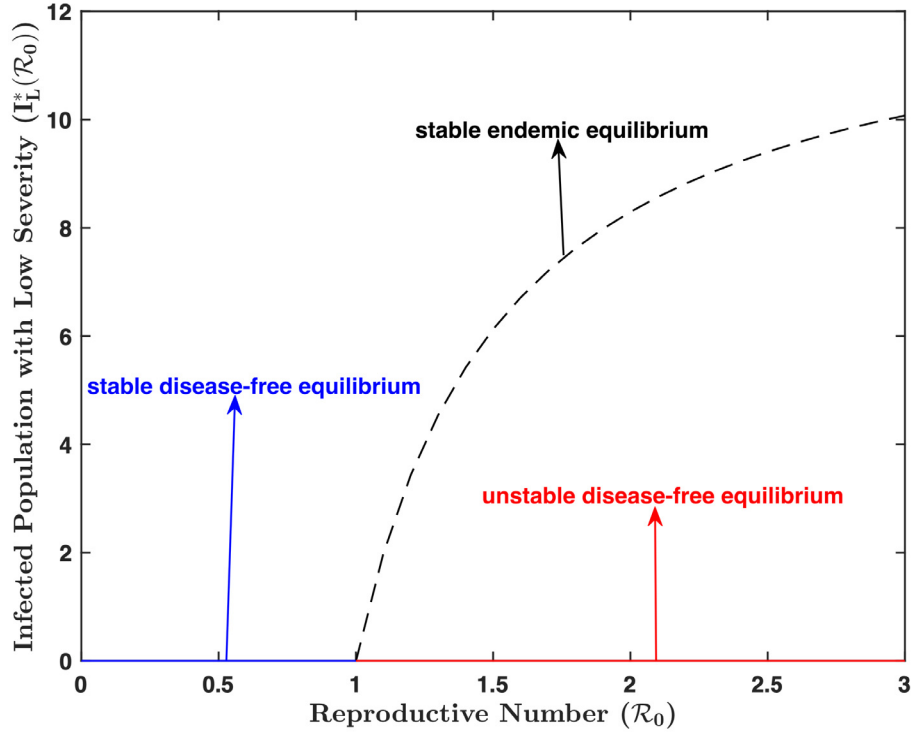


FIGURE 10. Bifurcation diagram for the model which shows an exchange of stability between disease-free and endemic equilibria at $\mathcal{R}_0 = 1$.

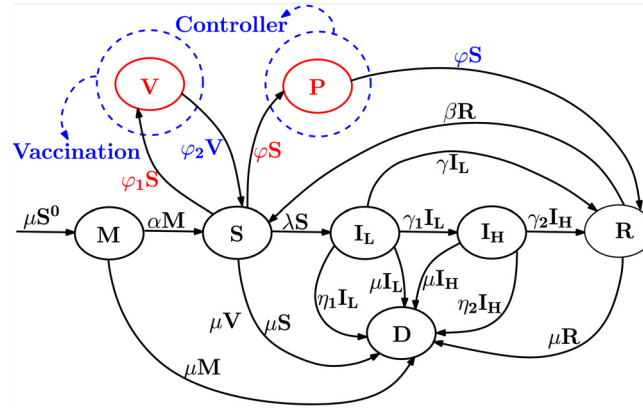


FIGURE 11. $MSI_L I_H R_V$ epidemic model for COVID-19 the with controller.

$$\begin{aligned}
 & -\varphi_1 (\gamma_1 + \gamma_2 + \gamma + \eta_1 + \eta_2 + \beta)) \mu^2 \\
 & + (((\gamma_1 + \gamma_2 + \eta_1 + \eta_2) \beta + (\gamma_2 + \eta_2) (\gamma + \gamma_1 + \eta_1)) \mathcal{R}_0 - \eta_1 \beta - (\gamma_1 + \eta_1) \eta_2 \\
 & - \eta_1 \gamma_2) \varphi_2 - ((\gamma_1 + \gamma_2 + \eta_1 + \eta_2) \beta + (\gamma_2 + \eta_2) (\gamma + \gamma_1 + \eta_1)) \varphi_1) \mu \\
 & + ((\gamma_1 + \eta_1) \eta_2 + \eta_1 \gamma_2) \beta ((\mathcal{R}_0 - 1) \varphi_2 - \varphi_1) (\alpha + \mu) \}^{-1}
 \end{aligned}$$

where \mathcal{M} is defined as follows,

$$\mathcal{M} = \mu S^0 (\beta + \mu) (\mu + \gamma_2 + \eta_2) (\mu \varphi_2 - \alpha ((\mathcal{R}_0 - 1) \varphi_2 - \varphi_1)),$$

with the production number of $\mathcal{R}_0 > 1$, the classical compartmental epidemic model includes just one endemic equilibrium. Moreover, the stability of the disease-free equilibrium is achieved by $\mathcal{R}_0 < 1$, while it is unstable when $\mathcal{R}_0 > 1$.

Figure 10 shows the bifurcation diagram so, that was obtained through numerical simulations using the relation $I_L^*(\mathcal{R}_0)$; it indicates an exchange of stability between the disease-free and endemic equilibria. If $\mathcal{R}_0 < 1$ the disease-free state is always the final reachable stable condition. When $\mathcal{R}_0 > 1$, the disease establishes itself in a community at endemic levels. This stability diagram confirms our analytic results; it shows that when $\mathcal{R}_0 > 1$, a stable endemic equilibrium exists; and when the same condition holds, the disease free becomes unstable.

3. OPTIMAL CONTROL STRATEGY TO CONTROL PANDEMIC COVID-19

Optimizing a system means minimizing or maximizing a function which measures the system performance. Three important steps to optimize of a system can be considered, (1) understanding the system and the various variables affecting it. (2) Selecting the functions as a measure of system performance. (3) Choosing the value for the system variables with optimizing the proposed system. Using an appropriate optimization method to obtain the optimal values is important [28, 33]. The aim of optimization is to obtain the efficient and best values for the parameters. Defining the convenient objective function is one of the most momentous steps of optimization [3, 40]. The most recent papers which provide mathematical models to control and predict the pandemic disease spreading about the COVID-19 disease are showed in the references [2, 16, 23, 39]. Figure 11 presents a flow chart of the proposed model with controller. This model was included the vaccination and protection covering classes. The optimal control strategy based on the $MSI_L I_H R_V$ model with protection covering is used. The objective function is included with the three classes of susceptible, infected and quarantined peoples. The aim is to find the maximum of number of susceptible people, minimum number of infected people, and the best value for of quarantine people.

$$\begin{cases} \frac{dM}{dt} = \mu S^0 - \alpha M - \mu M, \\ \frac{dS}{dt} = \alpha M + \varphi_2 \mathbf{V} + \beta R - \mu S - \lambda S - \varphi_1 S - \varphi \mathbf{S}, \\ \frac{dI_L}{dt} = \lambda S - \mu I_L - \eta_1 I_L - \gamma I_L - \gamma_1 I_L, \\ \frac{dI_H}{dt} = \gamma_1 I_L - \mu I_H - \eta_2 I_H - \gamma_2 I_H, \\ \frac{dR}{dt} = \gamma I_L + \gamma_2 I_H - \mu R - \beta R + \varphi \mathbf{S}, \\ \frac{dV}{dt} = \varphi_1 S - \varphi_2 \mathbf{V}, \\ \frac{dD}{dt} = \mu (M + S + I_L + I_H + R + V) + \eta_1 I_L + \gamma_2 I_H, \end{cases}$$

the objective function can be defined as,

$$J = \int_0^T \left[w_0 M(t) + w_1 S(t) + w_2 V(t) + w_3 I_L(t) + w_4 I_H(t) + du(t)^2 \right] dt; \quad t \in [0, T], \quad (3.1)$$

purpose of optimization is minimized or maximized the objective function (3.1), to determine the target variables with the following conditions,

$$\begin{aligned}
\dot{M} &= \mu S^0 - \alpha M - \mu M, \\
\dot{S} &= \alpha M + \varphi_2 \mathbf{V} + \beta R - \mu S - \lambda S - \varphi_1 S - \varphi \mathbf{S}, \\
\dot{I}_L &= \lambda S - \mu I_L - \eta_1 I_L - \gamma I_L - \gamma_1 I_L, \\
\dot{I}_H &= \gamma_1 I_L - \mu I_H - \eta_2 I_H - \gamma_2 I_H, \\
\dot{R} &= \gamma I_L + \gamma_2 I_H - \mu R - \beta R + \varphi \mathbf{S}, \\
\dot{V} &= \varphi_1 S - \varphi_2 \mathbf{V}, \\
\dot{D} &= \mu (M + S + I_L + I_H + R + V) + \eta_1 I_L + \gamma_2 I_H,
\end{aligned} \tag{3.2}$$

where, safekeeping coating rate of the susceptible people (φ) is defined as follows,

$$\varphi = uP,$$

where u is an utility function or controller (u is positive coefficient) and P is protection covering (information variable) [2, 3, 16, 17, 23, 28, 33, 39, 40]. Information about both the current and past condition of pandemic COVID-19 can be defined by the following formula,

$$P = \int_0^t \beta \times I_L \times S \times \frac{1}{\bar{\tau}} \times e\left(-\frac{t-\tau}{\bar{\tau}}\right) d\tau,$$

here, τ and $\bar{\tau}$ are the distributed delay and mean of the gathered information for the pandemic COVID-19, respectively [33]. Thus, model (3.1) can be reformulated to presents the diffusion model for the pandemic COVID-19 as the follows,

$$\begin{aligned}
\dot{M} &= \mu S^0 - \alpha M - \mu M, \\
\dot{S} &= \alpha M + \varphi_2 \mathbf{V} + \beta R - \mu S - \beta S I_L - \varphi_1 S - \mathbf{u} P \mathbf{S}, \\
\dot{I}_L &= \beta S I_L - \mu I_L - \eta_1 I_L - \gamma I_L - \gamma_1 I_L, \\
\dot{I}_H &= \gamma_1 I_L - \mu I_H - \eta_2 I_H - \gamma_2 I_H, \\
\dot{R} &= \gamma I_L + \gamma_2 I_H - \mu R - \beta R + \mathbf{u} P \mathbf{S}, \\
\dot{V} &= \varphi_1 S - \varphi_2 \mathbf{V}, \\
\dot{D} &= \mu (M + S + I_L + I_H + R + V) + \eta_1 I_L + \gamma_2 I_H, \\
\dot{P} &= \frac{1}{\bar{\tau}} (\beta S I_L - P),
\end{aligned} \tag{3.3}$$

System (3.2) has a virus absenteeism equilibrium, $VAE : (M^0, S^0, V^0, I_L^0, I_H^0, R^0, P^0) = \left(\frac{\mu S^0}{\alpha + \mu}, \frac{\alpha S^0}{\alpha + \mu}, \frac{\alpha \varphi_1 S^0}{\varphi_2 (\alpha + \mu)}, 0, 0, 0, 0 \right)$, and Jacobian matrix for the linearized system (3.2) around the virus absenteeism

equilibrium can be defined as follows,

$$J(\text{VAE}) = \begin{bmatrix} \frac{\partial F_i}{\partial M} & \frac{\partial F_i}{\partial S} & \frac{\partial F_i}{\partial V} & \frac{\partial F_i}{\partial I_L} & \frac{\partial F_i}{\partial I_H} & \frac{\partial F_i}{\partial R} & \frac{\partial F_i}{\partial P} \\ -\alpha - \mu & 0 & 0 & 0 & 0 & 0 & 0 \\ \alpha & -\mu - \varphi_1 - uP & \varphi_2 & -cp & 0 & \beta & -uS \\ 0 & 0 & 0 & cp - \mathcal{K} & 0 & 0 & 0 \\ 0 & 0 & 0 & \gamma_1 & 0 & 0 & 0 \\ 0 & 0 & 0 & \gamma & -\mu - \gamma_2 - \eta_2 & -\mu - \beta & 0 \\ 0 & \varphi_1 & -\varphi_2 & 0 & \gamma_2 & 0 & 0 \\ 0 & \beta/\bar{\tau}I_L & 0 & \beta/\bar{\tau}S & 0 & 0 & -1/\bar{\tau} \end{bmatrix},$$

with $\mathcal{K} = \mu + \gamma + \gamma_1 + \eta_1$. Transmission and transition matrixes F and V , along with the VAE in the proposed Jacobian matrix respectively can be found as follows,

$$F = \begin{bmatrix} 0 & 0 & 0 & 0 & 0 & 0 & 0 \\ \alpha & 0 & \varphi_2 & 0 & 0 & \beta & 0 \\ 0 & 0 & 0 & cp & 0 & 0 & 0 \\ 0 & 0 & 0 & \gamma_1 & 0 & 0 & 0 \\ 0 & 0 & 0 & \gamma & 0 & 0 & 0 \\ 0 & \varphi_1 & 0 & 0 & \gamma_2 & 0 & 0 \\ 0 & \beta/\bar{\tau}I_L & 0 & \beta/\bar{\tau}S & 0 & 0 & 0 \end{bmatrix},$$

and

$$V = \begin{bmatrix} -\alpha - \mu & 0 & 0 & 0 & 0 & 0 & 0 \\ 0 & -\mu - \varphi_1 - uP & 0 & -cp & 0 & \beta & -uS \\ 0 & 0 & 0 & -\mathcal{K} & 0 & 0 & 0 \\ 0 & 0 & 0 & 0 & -\mu - \gamma_2 - \eta_2 & 0 & 0 \\ 0 & 0 & 0 & 0 & 0 & -\mu - \gamma_2 - \eta_2 & 0 \\ 0 & 0 & -\varphi_2 & 0 & 0 & 0 & 0 \\ 0 & 0 & 0 & 0 & 0 & 0 & -1/\bar{\tau} \end{bmatrix},$$

where, F is a nonnegative matrix, V is a non-singular matrix and we have $J(\text{VAE}) = F - V$. Therefore, the reproductive number, \mathcal{R}_0 , is equal to the spectral radius $\rho(FV^{-1})$. Matrix V^{-1} , inverse of matrix V is giving by,

$$V^{-1} = \begin{bmatrix} -\frac{1}{\alpha + \mu} & 0 & 0 & 0 & 0 & 0 & 0 \\ 0 & -\frac{1}{\mu + \varphi_1 + uP} & \frac{cp}{\mathcal{K}(\mu + \varphi_1 + uP)} & 0 & 0 & 0 & \frac{\bar{\tau}uS}{\mu + \varphi_1 + uP} \\ 0 & 0 & 0 & 0 & 0 & -\frac{1}{\varphi_2} & 0 \\ 0 & 0 & -\frac{1}{\mathcal{K}} & 0 & 0 & 0 & 0 \\ 0 & 0 & 0 & -\frac{1}{\mu + \gamma_2 + \eta_2} & 0 & 0 & 0 \\ 0 & 0 & -\varphi_2 & 0 & 0 & -\frac{1}{\mu + \beta} & 0 \\ 0 & 0 & 0 & 0 & 0 & 0 & \bar{\tau} \end{bmatrix},$$

therefore, the reproductive number \mathcal{R}_0 is deriving as follows,

$$\begin{aligned} \mathcal{R}_0 &= \rho(FV^{-1}) = \rho \left(\begin{bmatrix} -\frac{\alpha}{\alpha+\mu} & 0 & 0 & 0 & 0 & 0 & 0 \\ 0 & 0 & 0 & 0 & -\frac{\beta}{\mu+\beta} & -1 & 0 \\ 0 & 0 & -\frac{cP}{\mathcal{K}} & 0 & 0 & 0 & 0 \\ 0 & 0 & -\frac{\gamma_1}{\mathcal{K}} & 0 & 0 & 0 & 0 \\ 0 & 0 & -\frac{\gamma}{\mathcal{K}} & -\frac{\gamma_2}{\mu+\gamma_2+\eta_2} & 0 & 0 & 0 \\ 0 & -\frac{\varphi_1}{\mu+\varphi_1+uP} & \frac{\varphi_1 cP}{\mathcal{K}(\mu+\varphi_1+uP)} & 0 & 0 & 0 & \frac{\bar{\tau}\varphi_1 uS}{\mu+\varphi_1+uP} \\ 0 & -\frac{\beta I_L}{\bar{\tau}(\mu+\varphi_1+uP)} & \frac{\beta cP I_L - \beta S(\mu+\varphi_1+uP)}{\bar{\tau}\mathcal{K}(\mu+\varphi_1+uP)} & 0 & 0 & 0 & \frac{\beta u I_L S}{\mu+\varphi_1+uP} \end{bmatrix} \right) \\ &= \max \left\{ \mathcal{Y}_1 = \frac{cP}{\mu + \gamma + \gamma_1 + \eta_1}, \mathcal{Y}_2 = \frac{\beta u I_L S - \mathbb{G}}{2(\mu + \varphi_1 + uP)}, \mathcal{Y}_3 = \frac{\beta u I_L S + \mathbb{G}}{2(\mu + \varphi_1 + uP)}, \mathcal{Y}_4 = 0, \mathcal{Y}_5 \right. \\ &= 0, \mathcal{Y}_6 = 0, \mathcal{Y}_7 = 0 \left. \right\}, \end{aligned}$$

with, $\mathbb{G} = \sqrt{(\beta u I_L S)^2 + 4\varphi_1 u P + 4\mu\varphi_1 + 4\varphi_1^2}$. Since, in the virus absenteeism equilibrium point the values of I_L and P are zero, then the eigenvalues of \mathcal{Y}_2 and \mathcal{Y}_3 can simplify as the follows,

$$\begin{aligned} \mathcal{Y}_2 &= \frac{\sqrt{4\mu\varphi_1 + 4\varphi_1^2}}{2(\mu + \varphi_1)} = \frac{\sqrt{\mu\varphi_1 + \varphi_1^2}}{\mu + \varphi_1} = \frac{\sqrt{\varphi_1(\mu + \varphi_1)}}{\mu + \varphi_1} = \sqrt{\frac{\varphi_1}{\mu + \varphi_1}}, \\ \mathcal{Y}_3 &= -\frac{\sqrt{4\mu\varphi_1 + 4\varphi_1^2}}{2(\mu + \varphi_1)} = -\frac{\sqrt{\mu\varphi_1 + \varphi_1^2}}{\mu + \varphi_1} = -\frac{\sqrt{\varphi_1(\mu + \varphi_1)}}{\mu + \varphi_1} = -\sqrt{\frac{\varphi_1}{\mu + \varphi_1}}, \end{aligned}$$

therefore, we have,

$$\begin{aligned} \mathcal{R}_0 &= \max \left\{ \mathcal{Y}_1 = \frac{cP}{\mu + \gamma + \gamma_1 + \eta_1}, \mathcal{Y}_2 = \sqrt{\frac{\varphi_1}{\mu + \varphi_1}} < 1, \mathcal{Y}_3 = -\sqrt{\frac{\varphi_1}{\mu + \varphi_1}} < 1 \right\} \\ &= \frac{cP}{\mu + \gamma + \gamma_1 + \eta_1}. \end{aligned}$$

To optimize the equation (3.1) with the conditions (3.2), we gain the Lagrangian and Hamiltonian functions [35] as follows,

Lagrangian: $\mathcal{L}(M, S, V, I_L, I_H) = w_0 M(t) + w_1 S(t) + w_2 V(t) + w_3 I_L(t) + w_4 I_H(t) + \mathbf{d}\mathbf{u}(t)^2$,

Hamiltonian: $\mathcal{H} = \mathcal{L}(M, S, V, I_L, I_H) + \Pi_1(t) \frac{dM}{dt} + \Pi_2(t) \frac{dS}{dt} + \Pi_3(t) \frac{dV}{dt} + \Pi_4(t) \frac{dI_L}{dt} + \Pi_5(t) \frac{dI_H}{dt} + \Pi_6(t) \frac{dR}{dt} + \Pi_7(t) \frac{dD}{dt} + \Pi_8(t) \frac{dP}{dt}$.

the Hamiltonian function can be rewritten as,

$$\begin{aligned} \mathcal{H} &= w_0 M(t) + w_1 S(t) + w_2 V(t) + w_3 I_L(t) + w_4 I_H(t) + \mathbf{d}\mathbf{u}(t)^2 \\ &+ \Pi_1(t) [\mu S^0 - \alpha M(t) - \mu M(t)] \\ &+ \Pi_2(t) [\alpha M(t) + \varphi_2 \mathbf{V}(t) + \beta R(t) - \mu S(t) - \beta S(t) I_L(t) - \varphi_1 S(t) \\ &- \mathbf{u}\mathbf{P}(t)\mathbf{S}(t)] + \Pi_3(t) [\varphi_1 S(t) - \varphi_2 \mathbf{V}(t)] \\ &+ \Pi_4(t) [\beta S(t) I_L(t) - \mu I_L(t) - \eta_1 I_L(t) - \gamma I_L(t) - \gamma_1 I_L(t)] \\ &+ \Pi_5(t) [\gamma_1 I_L(t) - \mu I_H(t) - \eta_2 I_H(t) - \gamma_2 I_H(t)] \\ &+ \Pi_6(t) [\gamma I_L(t) + \gamma_2 I_H(t) - \mu R(t) - \beta R(t) + \mathbf{u}\mathbf{P}(t)\mathbf{S}(t)] \\ &+ \Pi_7(t) [\mu (M(t) + S(t) + I_L(t) + I_H(t) + R(t) + V(t)) + \eta_1 I_L(t) + \gamma_2 I_H(t)] \\ &+ \Pi_8(t) \left[\frac{1}{\bar{\tau}} (\beta S(t) I_L(t) - P(t)) \right], \end{aligned}$$

where, Π'_i ($i = 1 \dots 8$) are the adjoint functions [22], and the adjoint equations for Π'_i s are given by,

$$\begin{aligned} \frac{d\Pi_1}{dt} &= -\frac{d\mathcal{H}}{dM} = -(w_0 - \alpha\Pi_1 - \mu\Pi_1 + \alpha\Pi_2 + \mu\Pi_7), \\ \frac{d\Pi_2}{dt} &= -\frac{d\mathcal{H}}{dS} = -\left(w_1 - \mu\Pi_2 - \beta I_L \Pi_2 - \varphi_1 \Pi_2 - uP\Pi_2 + \varphi_1 \Pi_3 + \beta I_L \Pi_4 + uP\Pi_6 + \mu\Pi_7 + \frac{\beta}{\tau} I_L \Pi_8\right), \\ \frac{d\Pi_3}{dt} &= -\frac{d\mathcal{H}}{dV} = -(w_2 + \varphi_2 \Pi_2 - \varphi_2 \Pi_3 + \mu\Pi_7), \\ \frac{d\Pi_4}{dt} &= -\frac{d\mathcal{H}}{dI_L} = -\left(w_3 - \beta S \Pi_2 + \beta S \Pi_4 - (\mu + \gamma + \gamma_1 + \eta_1) \Pi_4 + \gamma_1 \Pi_5 + \gamma \Pi_6 + (\mu + \eta_1) \Pi_7 + \frac{\beta}{\tau} S \Pi_8\right), \\ \frac{d\Pi_5}{dt} &= -\frac{d\mathcal{H}}{dI_H} = -(w_4 - (\mu + \gamma_2 + \eta_2) \Pi_5 + \gamma_2 \Pi_6 + (\mu + \gamma_2) \Pi_7), \\ \frac{d\Pi_6}{dt} &= -\frac{d\mathcal{H}}{dR} = -(\beta \Pi_2 - (\mu + \beta) \Pi_6 + \mu \Pi_7), \\ \frac{d\Pi_7}{dt} &= -\frac{d\mathcal{H}}{dD} = 0, \\ \frac{d\Pi_8}{dt} &= -\frac{d\mathcal{H}}{dP} = -\left(uS\Pi_6 - uS\Pi_2 - \frac{1}{\tau} \Pi_8\right), \end{aligned}$$

with the conditions $\Pi_i(T) = 0$ ($i = 1 \dots 8$)(transversally conditions). Using the Hamiltonian function the optimal utility function $u^*(t)$ can be derived as follows,

$$\frac{\partial \mathcal{H}}{\partial u} = \frac{1}{2} du - \Pi_2 PS + \Pi_6 PS = 0, \quad \implies \quad u^*(t) = \frac{\Pi_2(t) P^*(t) S^*(t) - \Pi_6(t) P^*(t) S^*(t)}{2d}.$$

using the exclusivity of control region, we gain,

$$u^*(t) = \max \left\{ \min \left\{ \frac{\Pi_2(t) P^*(t) S^*(t) - \Pi_6(t) P^*(t) S^*(t)}{2d}, 1 \right\}, 0 \right\}$$

the optimal points $M^*, S^*, V^*, I_L^*, I_H^*, R^*, D^*$ and P^* can be defined as follows,

$$\begin{aligned} \frac{dM^*}{dt} &= \mu S^0 - \alpha M^* - \mu M^*, \\ \frac{dS^*}{dt} &= \alpha M^* + \varphi_2 V^* + \beta R^* - \mu S^* - \beta S^* I_L^* - \varphi_1 S^* - u P^* S^* \\ \frac{dI_L^*}{dt} &= \beta S^* I_L^* - \mu I_L^* - \eta_1 I_L^* - \gamma I_L^* - \gamma_1 I_L^*, \\ \frac{dI_H^*}{dt} &= \gamma_1 I_L^* - \mu I_H^* - \eta_2 I_H^* - \gamma_2 I_H^*, \\ \frac{dR^*}{dt} &= \gamma I_L^* + \gamma_2 I_H^* - \mu R^* - \beta R^* + u P^* S^*, \\ \frac{dV^*}{dt} &= \varphi_1 S^* - \varphi_2 V^*, \\ \frac{dD^*}{dt} &= \mu (M^* + S^* + I_L^* + I_H^* + R^* + V^*) + \eta_1 I_L^* + \gamma_2 I_H^*, \\ \frac{dP^*}{dt} &= \frac{1}{\tau} (\beta S^* I_L^* - P^*), \end{aligned}$$

hence, optimal Hamiltonian can be defined as follows,

$$\begin{aligned} \mathcal{H}^* = & w_0 M^* + w_1 S^* + w_2 V^* + w_3 I_L^* + w_4 I_H^* + d \left\{ \max \left\{ \min \left\{ \frac{(\Pi_2 - \Pi_6) P^* S^*}{2d}, 1 \right\}, 0 \right\} \right\}^2 \\ & + \Pi_1 [\mu S^0 - \alpha M^* - \mu M^*] \\ & + \Pi_2 \left[\alpha M^* + \varphi_2 V^* + \beta R^* - \mu S^* - \beta S^* I_L^* - \varphi_1 S^* \right. \\ & \left. - \left\{ \max \left\{ \min \left\{ \frac{(\Pi_2 - \Pi_6) P^* S^*}{2d}, 1 \right\}, 0 \right\} \right\} P^* S^* \right] + \Pi_3 [\varphi_1 S^* - \varphi_2 V^*] \\ & + \Pi_4 [\beta S^* I_L^* - \mu I_L^* - \eta_1 I_L^* - \gamma I_L^* - \gamma_1 I_L^*] + \Pi_5 [\gamma_1 I_L^* - \mu I_H^* - \eta_2 I_H^* - \gamma_2 I_H^*] \\ & + \Pi_6 \left[\gamma I_L^* + \gamma_2 I_H^* - \mu R^* - \beta R^* + \left\{ \max \left\{ \min \left\{ \frac{(\Pi_2 - \Pi_6) P^* S^*}{2d}, 1 \right\}, 0 \right\} \right\} P^* S^* \right] \\ & + \Pi_7 [\mu (M^* + S^* + I_L^* + I_H^* + R^* + V^*) + \eta_1 I_L^* + \gamma_2 I_H^*] + \Pi_8 [1/\bar{\tau} (\beta S^* I_L^* - P^*)], \end{aligned}$$

4. PROGRAMMING ALGORITHM OF THE PROPOSED METHOD

First order derivative limitation definition has been used to program of the proposed method,

$$\mathbb{F}'(t) = \lim_{\Delta t \rightarrow 0} \frac{\mathbb{F}(t + \Delta t) - \mathbb{F}(t)}{\Delta t}, \quad (4.1)$$

algorithms of the presented methods by using definition (4.1), are given by:

$$\begin{bmatrix} M_{n+1} \\ S_{n+1} \\ I_{L,n+1} \\ I_{H,n+1} \\ R_{n+1} \\ V_{n+1} \\ D_{n+1} \\ P_{n+1} \end{bmatrix} = \begin{bmatrix} M_n \\ S_n \\ I_{L,n} \\ I_{H,n} \\ R_n \\ V_n \\ D_n \\ P_n \end{bmatrix} + \hbar \left(\begin{bmatrix} \mu S_n^0 \\ 0 \\ 0 \\ 0 \\ 0 \\ 0 \\ 0 \\ 0 \end{bmatrix} + \begin{bmatrix} -\mu - \alpha & 0 & 0 & 0 & 0 & 0 & 0 & 0 \\ \alpha & -\mu - \varphi_1 & -\beta S_n & 0 & \beta & \varphi_2 & 0 & -u S_n \\ 0 & \beta_n I_{L,n} & -\mathcal{K} & 0 & 0 & 0 & 0 & 0 \\ 0 & 0 & \gamma_1 & -\mu - \gamma_2 - \eta_2 & 0 & 0 & 0 & 0 \\ 0 & u P_n & \gamma & \gamma_2 & -\mu - \beta & 0 & 0 & 0 \\ 0 & \varphi_1 & -\varphi_2 & 0 & 0 & 0 & 0 & 0 \\ \mu & \mu & \mu & \mu + \eta_1 & \eta + \gamma_2 & \mu & 0 & 0 \\ 0 & \beta_n / \bar{\tau} I_{L,n} & 0 & 0 & 0 & 0 & 0 & 1/\bar{\tau} \end{bmatrix} \times \begin{bmatrix} M_n \\ S_n \\ I_{L,n} \\ I_{H,n} \\ R_n \\ V_n \\ D_n \\ P_n \end{bmatrix} \right),$$

with $\beta_n = cp/N_n$ and $\hbar = (t_n - t_0)/\mathcal{M}$ (\mathcal{M} stands as the number of iterations in the interval $[t_0, t_n]$).

$$\begin{bmatrix} \Pi_{1,n+1} \\ \Pi_{2,n+1} \\ \Pi_{3,n+1} \\ \Pi_{4,n+1} \\ \Pi_{5,n+1} \\ \Pi_{6,n+1} \\ \Pi_{7,n+1} \\ \Pi_{8,n+1} \end{bmatrix} = \begin{bmatrix} \Pi_{1,n} \\ \Pi_{2,n} \\ \Pi_{3,n} \\ \Pi_{4,n} \\ \Pi_{5,n} \\ \Pi_{6,n} \\ \Pi_{7,n} \\ \Pi_{8,n} \end{bmatrix} + \hbar \left(\begin{bmatrix} -w_0 \\ -w_1 \\ -w_2 \\ -w_3 \\ -w_4 \\ 0 \\ 0 \\ 0 \end{bmatrix} + \begin{bmatrix} \alpha + \mu & \alpha & 0 & 0 & 0 & \mu & 0 \\ 0 & \varphi_n & -\varphi_1 & -\beta_n I_{L,n} & 0 & -u P_n & -\mu & -\beta_n / \bar{\tau} I_{L,n} \\ 0 & -\varphi_2 & \varphi_2 & 0 & 0 & 0 & -1 & 0 \\ 0 & \beta S_n & 0 & \mathcal{K} - \beta_n S_n & -\gamma_1 & -\gamma & -\mu - \eta_1 & \beta_n / \bar{\tau} S_n \\ 0 & 0 & 0 & 0 & \mathcal{L} & -\gamma_2 & -\mu - \gamma_2 & 0 \\ 0 & -\beta & 0 & 0 & 0 & \mu + \beta & -\mu & 0 \\ \eta & 0 & 0 & 0 & 0 & 0 & 0 & 0 \\ 0 & u S_n & 0 & 0 & 0 & -u S_n & 0 & 1/\bar{\tau} \end{bmatrix} \times \begin{bmatrix} \Pi_{1,n} \\ \Pi_{2,n} \\ \Pi_{3,n} \\ \Pi_{4,n} \\ \Pi_{5,n} \\ \Pi_{6,n} \\ \Pi_{7,n} \\ \Pi_{8,n} \end{bmatrix} \right),$$

where, $\varphi_n = \mu + \varphi_1 + \beta_n I_{L,n} + u P_n$ and $\mathcal{L} = \mu + \gamma_2 + \eta_2$. Hence, the optimal controller is given by,

$$u_n^* = \left\{ \max \left\{ \min \left\{ \frac{(\Pi_{2,n} - \Pi_{6,n}) P_n^* S_n^*}{2d}, 1 \right\}, 0 \right\} \right\}.$$

Optimal values of M^* , S^* , V^* , I_L^* , I_H^* , R^* , D^* and P^* can be obtained by solving the following optimal matrix equation,

$$\begin{bmatrix} M_{n+1}^* \\ S_{n+1}^* \\ V_{n+1}^* \\ I_{L,n+1}^* \\ I_{H,n+1}^* \\ R_{n+1}^* \\ D_{n+1}^* \\ P_{n+1}^* \end{bmatrix} = \begin{bmatrix} M_n^* \\ S_n^* \\ V_n^* \\ I_{L,n}^* \\ I_{H,n}^* \\ R_n^* \\ D_n^* \\ P_n^* \end{bmatrix} + \hbar \left(\begin{bmatrix} \mu S^0 \\ 0 \\ 0 \\ 0 \\ 0 \\ 0 \\ 0 \\ 0 \end{bmatrix} + \begin{bmatrix} -\mu - \alpha & 0 & 0 & 0 & 0 & 0 & 0 & 0 \\ \alpha & -\mu - \varphi_1 & -\beta_n^* S_n^* & 0 & \beta & \varphi_2 & 0 & -\mathbf{u}_n^* \mathbf{S}_n^* \\ 0 & \beta_n^* I_{L,n}^* & -\mathcal{K} & 0 & 0 & 0 & 0 & 0 \\ 0 & 0 & \gamma_1 & -\mu - \gamma_2 - \eta_2 & 0 & 0 & 0 & 0 \\ 0 & \mathbf{u}_n^* \mathbf{P}_n^* & \gamma & \gamma_2 & -\mu - \beta & 0 & 0 & 0 \\ 0 & \varphi_1 & -\varphi_2 & 0 & 0 & 0 & 0 & 0 \\ \eta & \mu & \mu & \mu + \eta_1 & \mu + \gamma_2 & \eta & 0 & 0 \\ 0 & \beta_n^* / \bar{\tau} I_{L,n}^* & 0 & 0 & 0 & 0 & 0 & 1/\bar{\tau} \end{bmatrix} \times \begin{bmatrix} M_n^* \\ S_n^* \\ V_n^* \\ I_{L,n}^* \\ I_{H,n}^* \\ R_n^* \\ D_n^* \\ P_n^* \end{bmatrix} \right),$$

with $\beta_n^* = cp/N_n$ and $\hbar = (t_n - t_0)/\mathcal{M}$ (\mathcal{M} is number of iterations in the interval $[t_0, t_n]$). After, obtained the optimal values of M_n^* , S_n^* , V_n^* , $I_{L,n}^*$, $I_{H,n}^*$, R_n^* , D_n^* , P_n^* and \mathbf{u}_n^* , the optimal Hamiltonian function \mathcal{H}_n^* can be derived as follows,

$$\begin{aligned} \mathcal{H}_n^* &= w_0 M_n^* + w_1 S_n^* + w_2 V_n^* + w_3 I_{L,n}^* + w_4 I_{H,n}^* + d\mathbf{u}_n^{*2} + \Pi_1 [\mu S^0 - \alpha M_n^* - \mu M_n^*] \\ &+ \Pi_2 [\alpha M_n^* + \varphi_2 V_n^* + \beta R_n^* - \mu S_n^* - \beta_n^* S_n^* I_{L,n}^* - \varphi_1 S_n^* - \mathbf{u}_n^* \mathbf{P}_n^* \mathbf{S}_n^*] \\ &+ \Pi_3 [\varphi_1 S_n^* - \varphi_2 V_n^*] + \Pi_4 [\beta_n^* S_n^* I_{L,n}^* - \mu I_{L,n}^* - \eta_1 I_{L,n}^* - \gamma I_{L,n}^* - \gamma_1 I_{L,n}^*] \\ &+ \Pi_5 [\gamma_1 I_{L,n}^* - \mu I_{H,n}^* - \eta_2 I_{H,n}^* - \gamma_2 I_{H,n}^*] \\ &+ \Pi_6 [\gamma I_{L,n}^* + \gamma_2 I_{H,n}^* - \mu R_n^* - \beta R_n^* + \mathbf{u}_n^* \mathbf{P}_n^* \mathbf{S}_n^*] \\ &+ \Pi_7 [\mu (M_n^* + S_n^* + I_{L,n}^* + I_{H,n}^* + R_n^* + V_n^*) + \eta_1 I_{L,n}^* + \gamma_2 I_{H,n}^*] \\ &+ \Pi_8 [1/\bar{\tau} (\beta_n^* S_n^* I_{L,n}^* - P_n^*)]. \end{aligned}$$

5. PROGRAMMING AND SIMULATION

Programming and simulation of proposed models is performed in this Section for the controller and without controller cases. The source of parameters and its numerical values are as follows [13],

$$\mu = 0.05, \alpha = 0.35, \varphi_1 = 0.25, \varphi_2 = 0.05, \beta = 0.2, \beta_1 = 0.15, \varphi = 0.05, \eta_1 = 0.03,$$

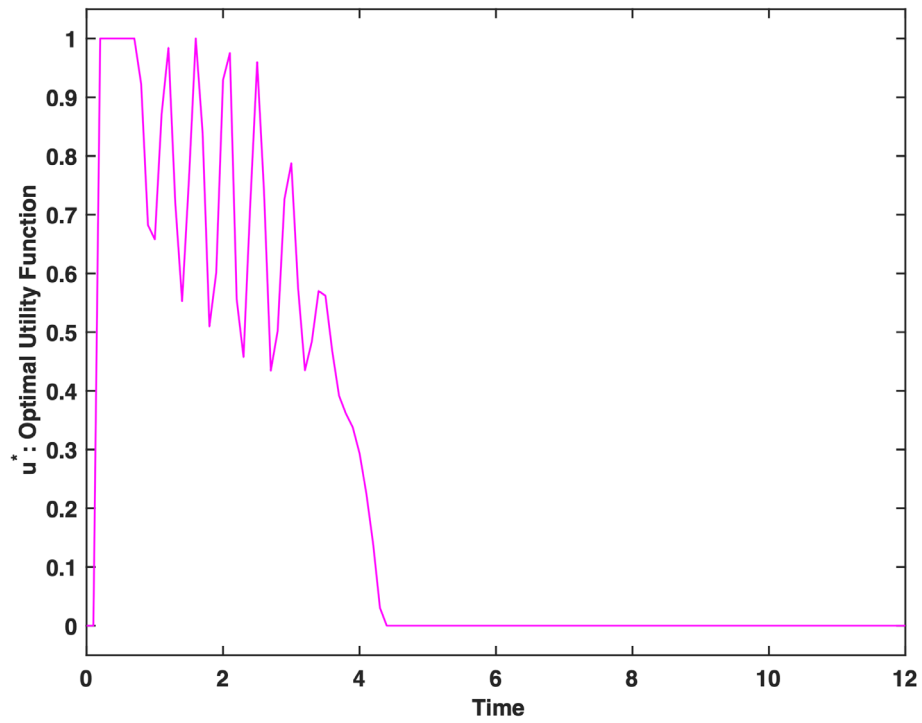
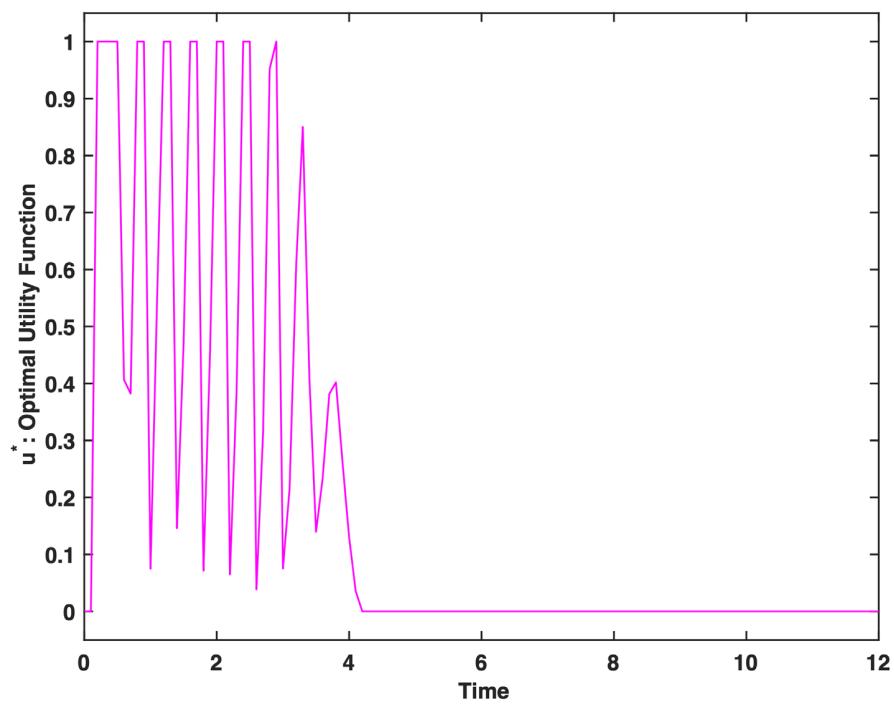
$$\eta_2 = 0.02, \gamma = 0.6, \gamma_1 = 0.08, \gamma_2 = 0.15, c = 4, p = 0.35, T = 5, S^0 = 800, M(0) = 50,$$

$$S(0) = 120, V(0) = 5, I_L(0) = 6, I_H(0) = 2, R(1) = 0, P(0) = 0, D(0) = 0, r = 0.5,$$

$$u_0 = 0.15, w_1 = w_2 = w_3 = w_4 = w_5 = w_6 = 0.1, \Pi_1(0) = \Pi_2(0) = \Pi_3(0) = \Pi_4(0)$$

$$= \Pi_5(0) = \Pi_6(0) = \Pi_7(0) = \Pi_8(0) = 0.01.$$

Figures 12–15 show the optimal controller function, $u^*(t)$, for $\beta = 0.1$, $\beta = 0.2$, $\beta = 0.3$ and $\beta = 0.4$, respectively. According to the figures, with the increase of the parameter β from 0.1 up to 0.4, the number of vibrations of the controller function also increases over time. The immunity people, $M(t)$, with controller and without controller for $\beta = 0.2$ is showed in the Figure 16. As it can be seen from the figure, the use of the controller in the proposed model has no effect on the immune individuals size.

FIGURE 12. Optimal utility function *vs.* time when $\beta = 0.1$.FIGURE 13. Optimal utility function *vs.* time when $\beta = 0.2$.

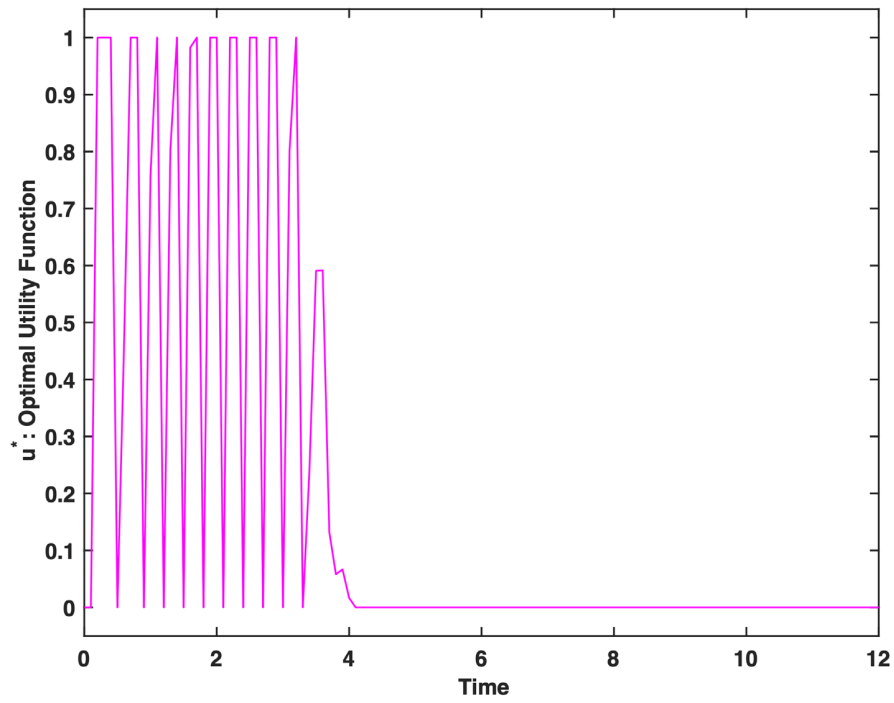


FIGURE 14. Optimal utility function *vs.* time when $\beta = 0.3$.

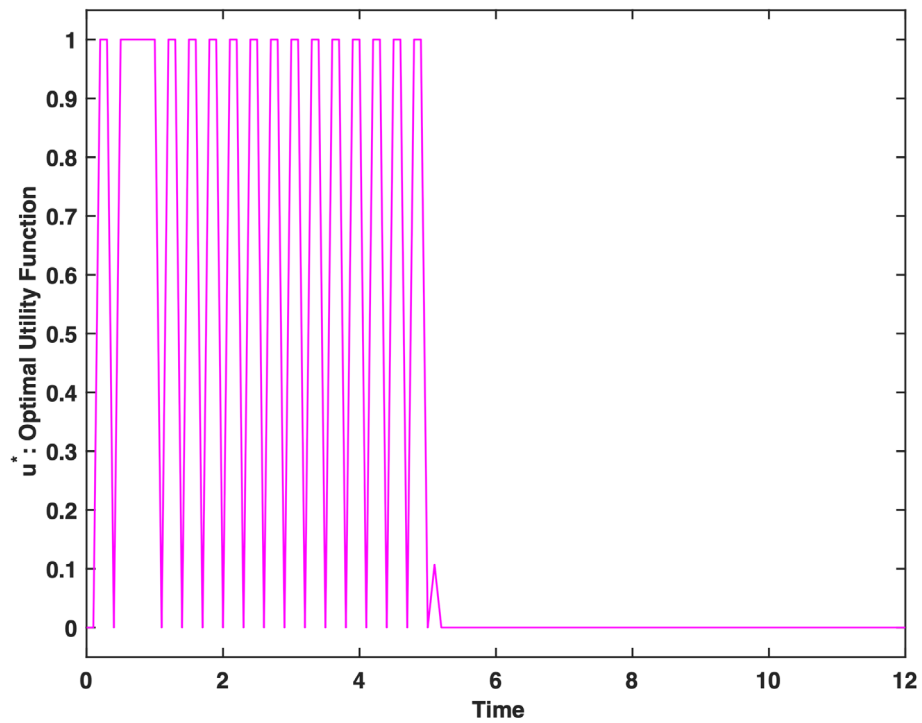
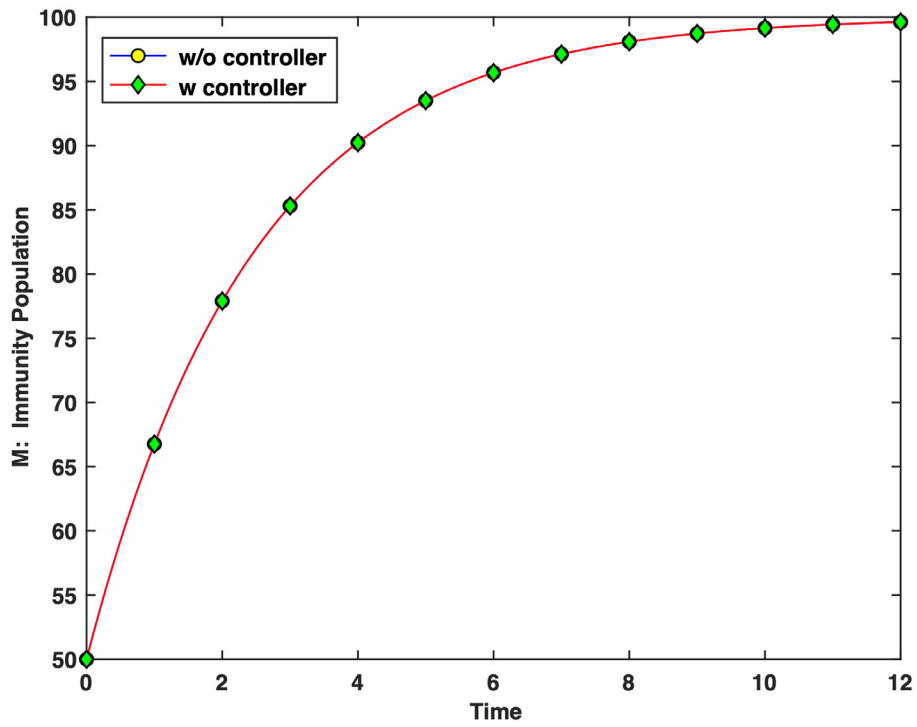
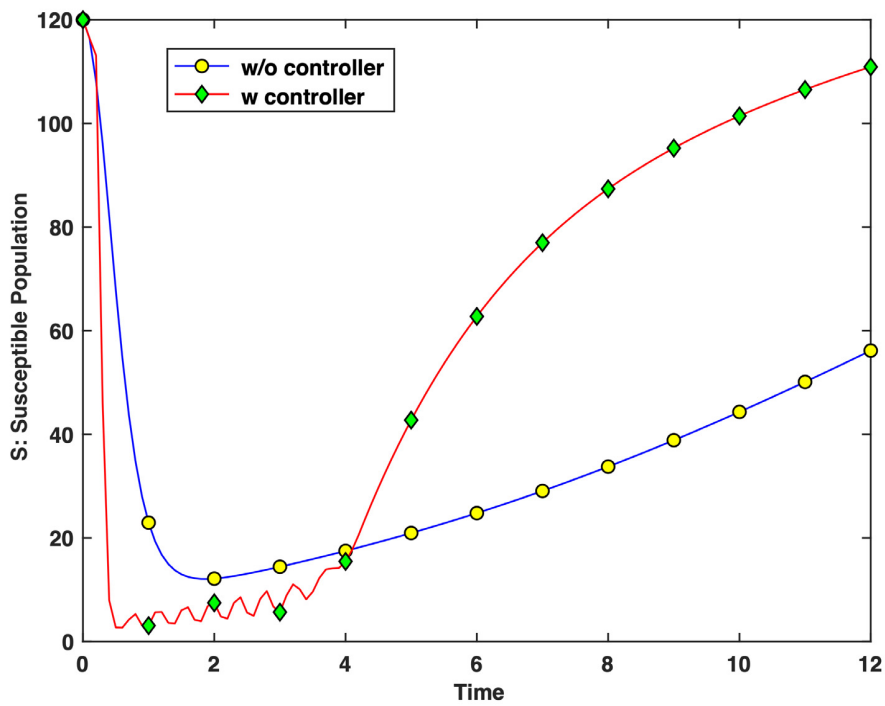


FIGURE 15. Optimal utility function *vs.* time when $\beta = 0.4$.

FIGURE 16. Immunity population *vs.* time when $\beta = 0.2$.FIGURE 17. Susceptible population *vs.* time when $\beta = 0.2$.

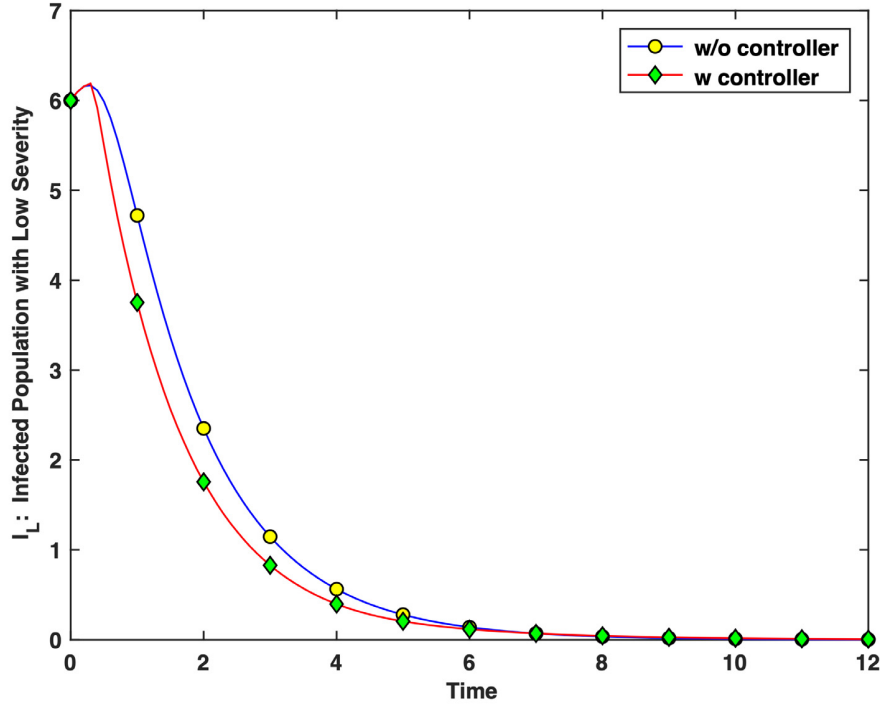


FIGURE 18. Infected population with low severity *vs.* time when $\beta = 0.2$.

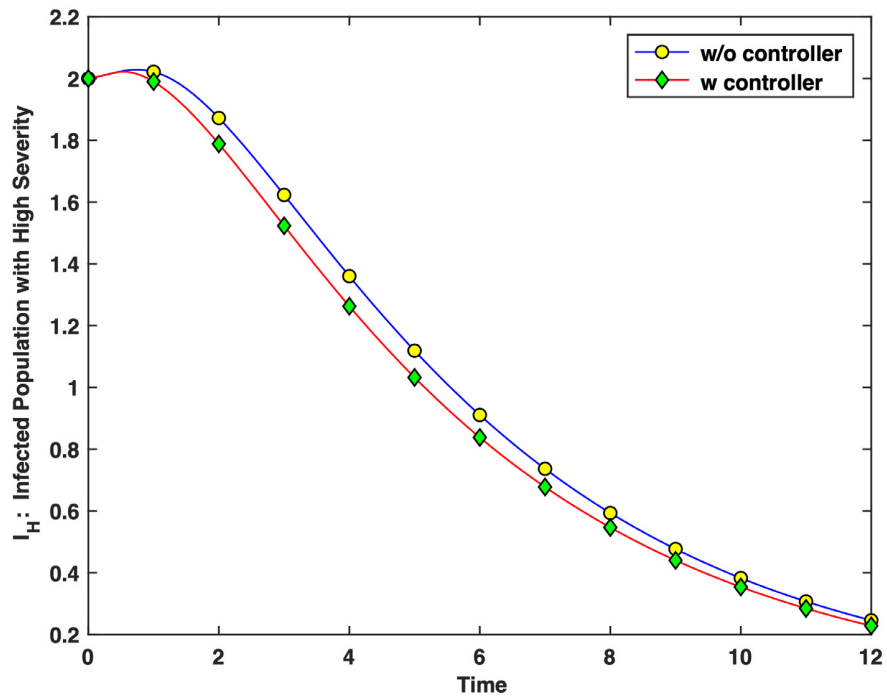
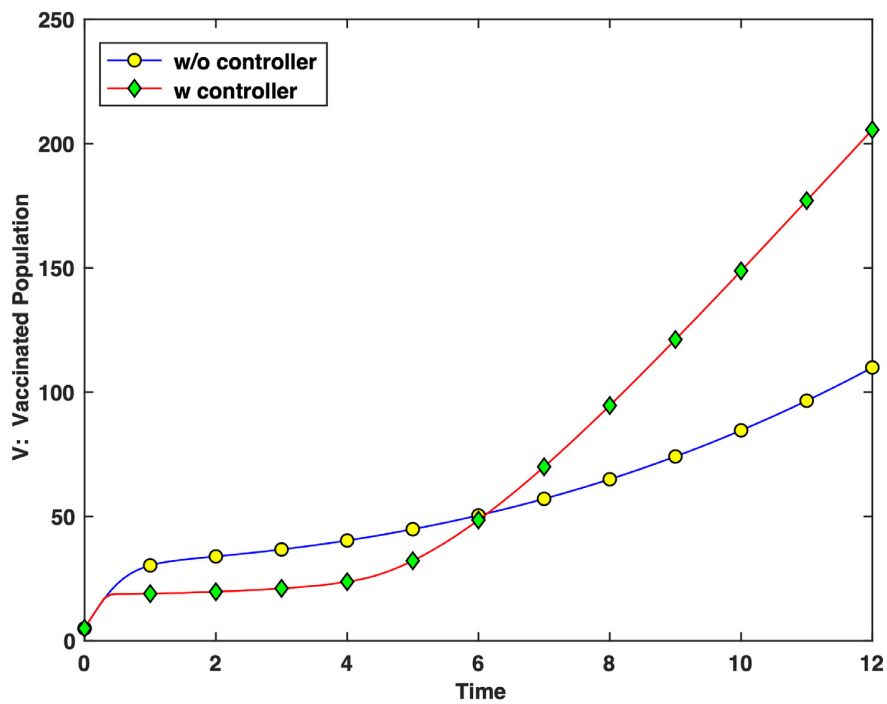
Figure 17 shows the susceptible people, $S(t)$, with controller and without controller for $\beta = 0.2$. As can be seen, using the utility function, the number of susceptible individuals increases outstandingly. The infected people with low and high severity, $I_L(t)$ and $I_H(t)$, with controller and without controller, are shown in the Figures 18 and 19 for $\beta = 0.2$. The use of the controller in the proposed model has caused the rate of the infected people to drop to zero more quickly. Figure 20, indicates the vaccinated individual's *vs.* time with controller and without controller when $\beta = 0.2$. The use of the controller in the proposed model shows that after a certain period of time we need to increase the number of vaccinated people. Figure 21 indicates the recovered people, $R(t)$, with controller and without controller for $\beta = 0.2$. It's depicted from this figure that in the proposed model, along with the controller, the recovered individuals increase more rapidly.

6. VALIDATION OF PROPOSED MODEL WITH THE REAL DATA

Table 1 shows the real data of COVID-19 from 4 January, 2021 up to 14 June, 2021 in Iran.¹ In the present section, we have used the real data to validate the proposed models with controller and without controller for infected individuals and dead peoples. According the Table 1, mean of infected peoples is $\bar{I} = \bar{I}_L + \bar{I}_H = 77,062$, mean of dead peoples is $\bar{D} = 1,142$, mean of infection rate is $\bar{\lambda} = 0.0346$ and mean of death rate is $\bar{\mu} = 0.0314$. Figure 22, indicates the optimal utility function *versus* time for the real data of COVID-19 from 4 Jan, 2021 up to 14 June, 2021 in Iran¹.

Infected population *versus* time for the real data of COVID-19 from 4 Jan, 2021 up to 14 June, 2021 in Iran¹ was shown in Figure 23. As seen from this figure, the infection population obtained from the model without controller has been fitted to the real data. As seen from this figure, the infected population using the proposed model without controller has been fitted to the real data. As can be seen, the use of the controller

¹<https://covid19.who.int/region/emro/country/ir>

FIGURE 19. Infected population with high severity *vs.* time when $\beta = 0.2$.FIGURE 20. Vaccinated population *vs.* time when $\beta = 0.2$.

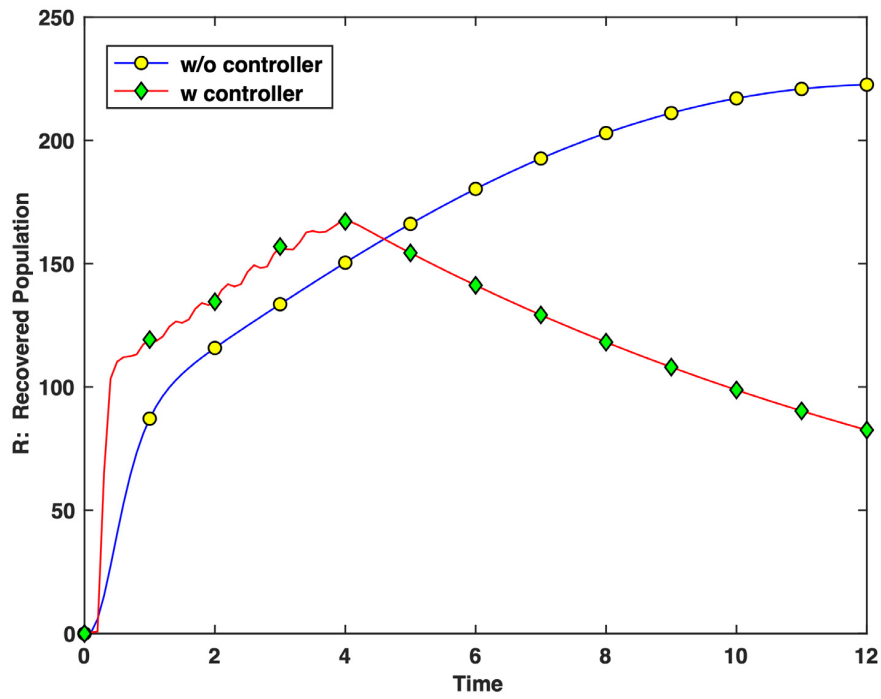


FIGURE 21. Recovered population *vs.* time when $\beta = 0.2$.

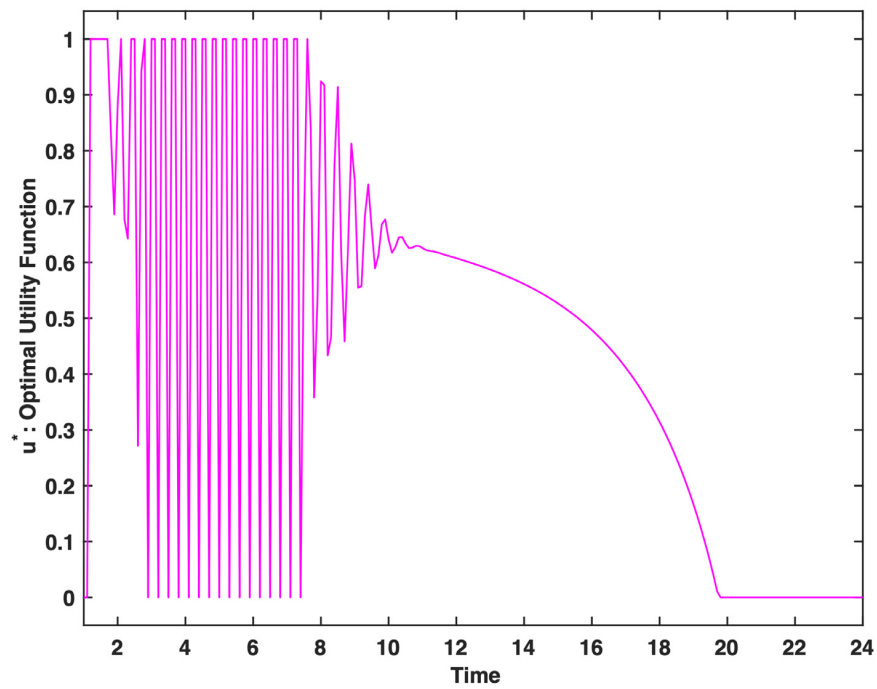


FIGURE 22. Optimal utility function *versus* time for the real data of COVID-19 from 4 Jan, 2021 up to 14 June, 2021 in Iran¹.

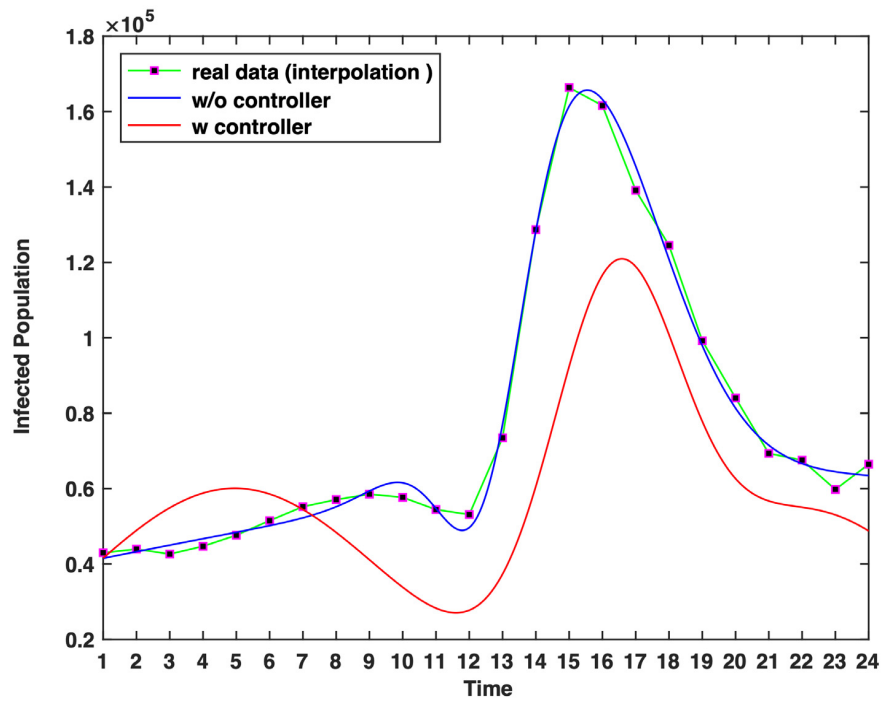


FIGURE 23. Infected population *versus* time for the real data (interpolation) of COVID-19 from 4 Jan, 2021 up to 14 June, 2021 in Iran¹.

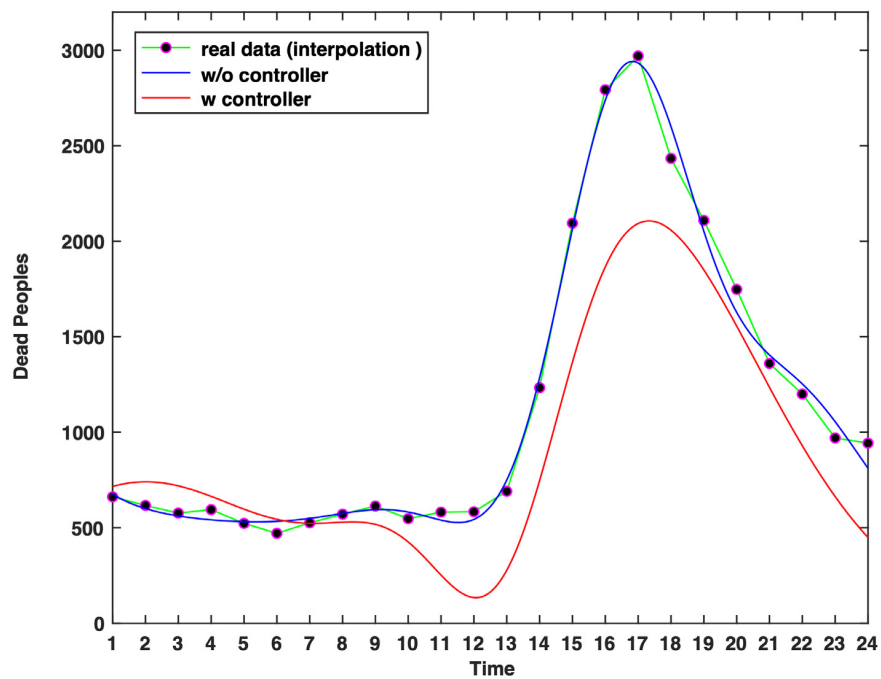


FIGURE 24. Dead population *versus* time for the real data (interpolation) of COVID-19 from 4 Jan, 2021 up to 14 June, 2021 in Iran¹.

TABLE 1. Real data of COVID-19 from 4 Jan, 2021 up to 14 June, 2021 in Iran¹.

Labels	Dates	Infected peoples	Weekly change (%)	Dead peoples	Weekly change (%)
1	4 Jan	42,964	1.07	662	-23.38
2	11 Jan	43,957	2.31	617	-6.80
3	18 Jan	42,637	-3.00	577	-6.48
4	25 Jan	44,699	4.84	595	3.12
5	1 Feb	47,639	6.58	523	-12.10
6	8 Feb	51,503	8.11	471	-9.94
7	15 Feb	55,208	7.19	526	11.68
8	22 Feb	57,078	3.39	571	8.56
9	1 March	58,523	2.53	614	7.53
10	8 March	57,678	-1.44	548	-10.75
11	15 March	54,445	-5.61	582	6.20
12	22 March	53,118	-2.44	584	0.34
13	29 March	73,471	38.32	691	18.32
14	5 Apr	128,684	75.15	1233	78.44
15	12 Apr	166,367	29.28	2095	69.91
16	19 Apr	161,594	-2.87	2793	33.32
17	26 Apr	139,118	-13.91	2970	6.34
18	3 May	124,513	-10.50	2434	-18.05
19	10 May	99,205	-20.33	2109	-13.35
20	17 May	84,012	-15.31	1748	-17.12
21	24 May	69,331	-17.47	1360	-22.20
22	31 May	67,533	-2.59	1200	-11.76
23	7 June	59,771	-11.49	970	-19.17
24	14 June	66,452	11.18	943	2.78
		$\bar{I} = \bar{I}_L + \bar{I}_H = 77,062$	$\bar{\lambda} = 0.0346$	$\bar{D} = 1,142$	$\bar{\mu} = 0.0314$

has significantly reduced the number of infected people and much better and more accurately optimized the infected people. It is worth mentioning, we applied an interpolation for the actual data's.

Figure 24, shows the dead population *versus* time for the real data of COVID-19 from 4 Jan, 2021 up to 14 June, 2021 in Iran¹. According the results of Figure 24, the dead population obtained from the proposed model without controller is almost consistent with the actual data. And use of controller efficiently and effectively has optimized the dead population. The use of the controller, better and more accurately optimized the dead people and significantly reduced the number of dead population.

7. CONCLUSION

In this paper, a mathematical model including classes M , S , V , I_L , I_H and R has been presented for the pandemic COVID-19. Disease-free equilibriums TE, VAE and VIE were derived to study the stability, criticality and instability of the proposed model for pandemic COVID-19. Using Jacobian matrix of dynamical system in the virus absenteeism equilibrium point, reproductive number was derived. Results showed that, the spectral radius of the new operator, using the transmission matrix and transition matrix as well as virus absenteeism equilibrium, was a very powerful tool to obtain the reproductive number. To control pandemic COVID-19 spread, the effect of vaccination and protective covering were studied. The results showed that by following the health and safety protocols such as wearing face masks, keeping proper distances from others, hand washing, using disinfectants, etc. might help a lot in controlling the infectious disease of COVID-19. In the following, optimal control theory is used to optimize the proposed model, for the prediction and the control of pandemic

COVID-19, and to improve the performance of the model. The results of the optimal control theory show that the optimal utility function could be extremely advantageous and effective in controlling infectious diseases. Validation of proposed methods with the real data shows that use of the controller in the epidemic COVID-19, efficiently and accurately has optimized the infected and dead populations and has significantly reduced the number of infected and dead peoples.

DECLARATION OF CONFLICTING INTERESTS

The author(s) declared no potential conflicts of interest with respect to the research, authorship, and/or publication of this article.

Acknowledgements. The authors would like to thank Tabriz Branch, Islamic Azad University for the financial support of this research, which is based on a research project contract.

REFERENCES

- [1] D. Adak, A. Majumder and N. Bairagi, Mathematical perspective of Covid-19 pandemic: Disease extinction criteria in deterministic and stochastic models. *Chaos Solitons Fractals* **142** (2021) 110381.
- [2] S.Ý. Araz, Analysis of a Covid-19 model: optimal control, stability and simulations. *Alexandria Eng. J.* **60** (2021) 647–658.
- [3] B.A. Baba and B. Bilgehan, Optimal control of a fractional order model for the COVID–19 pandemic. *Chaos Solitons Fract.* **144** (2021) 110678.
- [4] A. Baleta, Dramatic drop in SA’s immunization rates. Spotlight, 24 June 2020.
- [5] S.P. Blythe, C. Castillo-Chavez, J.S. Palmer and M. Cheng, Toward a unified theory of sexual mixing and pair formation. *Math. Biosci.* **107** (1991) 379–405.
- [6] S. Busenberg and C. Castillo-Chavez, Interaction pair formation and force of infection terms in sexually transmitted disease, in vol. 83 *Mathematical and Statistical Approaches to AIDS Epidemiology*, edited by Castillo-Chavez. Lecture Notes in Biomathematics. Springer-Verlag, New York (1989) 289–300.
- [7] K. Causey, N. Fullman, R.J. Sorensen, N.C. Galles, P. Zheng, A. Aravkin and J.F. Mosser, Estimating global and regional disruptions to routine childhood vaccine coverage during the COVID-19 pandemic in 2020: a modelling study. *The Lancet* (2021).
- [8] S. Chandir, D.A. Siddiqi, H. Setayesh and A.J. Khan, Impact of COVID-19 lockdown on routine immunisation in Karachi, Pakistan. *Lancet Global Health* **8** (2020) e1118–e1120.
- [9] S.S. Chaharborj, M. Rizam Abu Bakar and N. Akma Ibrahim, Deterministic and Stochastic Models for HIV. LAP Lambert Academic Publishing, Germany (2013).
- [10] S.S. Chaharborj, M.R.A. Bakar and A. Ebadian, Disease transmission MSEIR model with individuals traveling between patches i and $i + 1$. *J. Appl. Math. Inf.* **28** (2010) 1073–1088.
- [11] S.S. Chaharborj, M. Rizam Abu Bakar and N. Akma Ibrahim, Deterministic and Stochastic Models for HIV. LAP Lambert Academic Publishing, Germany (2013).
- [12] S.L. Chang, N. Harding, C. Zachreson, O.M. Cliff and M. Prokopenko, Modelling transmission and control of the COVID-19 pandemic in Australia. *Nat. Commun.* **11** (2020) 1–13.
- [13] S.S. Chaharborj, I. Fudziah, M.A. Bakar, R.S. Chaharborj, Z.A. Majid and A.G.B. Ahmad, The use of generation stochastic models to study an epidemic disease. *Adv. Differ. Equ.* **2013** (2013) 1–9.
- [14] S.S. Chaharborj, M.R.A. Bakar and A. Ebadian, Disease transmission MSEIR model with individuals traveling between patches i and $i + 1$. *J. Appl. Math. Inf.* **28** (2010) 1073–1088.
- [15] R. Chowdhury, K. Heng, M.S.R. Shawon, G. Goh, D. Okonofua, C. Ochoa-Rosales and O.H. Franco, Dynamic interventions to control COVID-19 pandemic: a multivariate prediction modelling study comparing 16 worldwide countries. *Eur. J. Epidemiol.* **35** (2020) 389–399.
- [16] C.T. Deressa and G.F. Duressa, Modeling and optimal control analysis of transmission dynamics of COVID-19: The case of Ethiopia. *Alexandria Eng. J.* **60** (2021) 719–732.
- [17] A. d’Onofrio and P. Manfredi, Bifurcation thresholds in an SIR model with information-dependent vaccination. *Math. Model. Natur. Phenom.* **2** (2007) 26–43.
- [18] O. Diekmann, J.A.P. Heesterbeek and J.A. Metz, On the definition and the computation of the basic reproduction ratio R_0 in models for infectious diseases in heterogeneous populations. *J. Math. Biol.* **28** (1990) 365–382.
- [19] O. Diekmann, J.A.P. Heesterbeek and J.A. Metz, On the definition and the computation of the basic reproduction ratio R_0 in models for infectious diseases in heterogeneous populations. *J. Math. Biol.* **28** (1990) 365–382.
- [20] L. Di Domenico, G. Pullano, C.E. Sabbatini, P.Y. Boëlle and V. Colizza, Modelling safe protocols for reopening schools during the COVID-19 pandemic in France. *Nat. Commun.* **12** (2021) 1–10.

- [21] L. Di Domenico, G. Pullano, C.E. Sabbatini, P.-Y. Boëlle and V. Colizza, Impact of lockdown on COVID-19 epidemic in Île-de-France and possible exit strategies. *BMC Med.* **18** (2020) 240.
- [22] P. Eichmeir, T. Lauß, S. Oberpeilsteiner, K. Nachbagauer and W. Steiner, The adjoint method for time-optimal control problems. *J. Comput. Nonlinear Dyn.* **16** (2021).
- [23] H. Ferjouchia, A. Kouidere, O. Zakary and M. Rachik, Optimal control strategy of COVID-19 spread in morocco using SEIRD model. *Moroccan J. Pure Appl. Anal.* **7** (2021) 66–79.
- [24] S. Flaxman *et al.*, Estimating the effects of non-pharmaceutical interventions on COVID-19 in Europe. *Nature* **584** (2020) 257–261.
- [25] N. Haug *et al.*, Ranking the effectiveness of worldwide COVID-19 government interventions. *Nat. Hum. Behav.* **4** (2020) 1303–1312.
- [26] H.W. Hethcote, The mathematics of infectious diseases. *SIAM Rev.* **42** (2000) 599–653.
- [27] S. Hsiang *et al.*, The effect of large-scale anti-contagion policies on the COVID-19 pandemic. *Nature* **584** (2020) 262–267.
- [28] N. Keshri and B.K. Mishra, Optimal control model for attack of worms in wireless sensor network. *Int. J. Grid Distrib. Comput.* **7** (2014) 251–272.
- [29] Z.S. Lassi, R. Naseem, R.A. Salam, F. Siddiqui and J.K. Das, The impact of the COVID-19 pandemic on immunization campaigns and programs: a systematic review. *Int. J. Environ. Res. Public Health* **18** (2021) 988.
- [30] P. Martens, How will climate change affect human health? *Am. Sci.* **87** (1999) 534–541.
- [31] B.G. Masresha, R. Luce Jr, M.E. Shibeshi, B. Ntsama, N’A. Diaye, J. Chakauya, and R. Mihigo, The performance of routine immunization in selected African countries during the first six months of the COVID-19 pandemic. *Pan Afri. Med. J.* **37** (2020).
- [32] K. Mulholland, K. Kretsinger, L. Wondwossen and N. Crowcroft, Action needed now to prevent further increases in measles and measles deaths in the coming years. *The Lancet* **396** (2020) 1782–1784.
- [33] P.A. Naik, J. Zu and K.M. Owolabi, Global dynamics of a fractional order model for the transmission of HIV epidemic with optimal control. *Chaos Solitons Fract.* **138** (2020) 109826.
- [34] National Health Commission (NHC) of the People’s Republic of China (2020). NHC daily reports. http://www.nhc.gov.cn/yjb/pzhgli/new_list.shtml.
- [35] F. Pegoraro and S.V. Bulanov, Nonlinear, nondispersive wave equations: Lagrangian and Hamiltonian functions in the hodograph transformation. *Phys. Lett. A* **384** (2020) 126064.
- [36] A. Raza, A. Ahmadian, M. Rafiq, S. Salahshour and M. Ferrara, An analysis of a nonlinear susceptible-exposed-infected-quarantine-recovered pandemic model of a novel coronavirus with delay effect. *Results Phys.* **2020** (2020) 103771.
- [37] A. Raza, A. Ahmadian, M. Rafiq, S. Salahshour and M. Ferrara, An analysis of a nonlinear susceptible-exposed-infected-quarantine-recovered pandemic model of a novel coronavirus with delay effect. *Results Phys.* **2020** (2020) 103771.
- [38] M.A. Shereen, S. Khan, A. Kazmi, N. Bashir and R. Siddique, COVID-19 infection: origin, transmission, and characteristics of human coronaviruses. *J. Adv. Res.* (2020).
- [39] C.J. Silva, C. Cruz, D.F. Torres, A.P. Muñuzuri, A. Carballosa, I. Area and J. Mira, Optimal control of the COVID-19 pandemic: controlled sanitary deconfinement in Portugal. *Sci. Rep.* **11** (2021) 1–15.
- [40] C. Tsay, F. Lejarza, M.A. Stadtherr and M. Baldea, Modeling, state estimation, and optimal control for the US COVID-19 outbreak. *Sci. Rep.* **10** (2020) 1–12.
- [41] P. Van den Driessche and J. Watmough, Reproduction numbers and sub-threshold endemic equilibria for compartmental models of disease transmission. *Math. Biosci.* **180** (2002) 29–48.
- [42] P.G. Walker, C. Whittaker, O. Watson *et al.*, The global impact of COVID-19 and strategies for mitigation and suppression. London: WHO Collaborating Centre for Infectious Disease Modelling, MRC Centre for Global Infectious Disease Analysis, Abdul Latif Jameel Institute for Disease and Emergency Analytics, Imperial College London (2020).
- [43] C. Wang, P.W. Horby, F.G. Hayden and G.F. Gao, A novel coronavirus outbreak of global health concern. *Lancet* **395** (2020) 470–473.
- [44] WHO, Report of the WHO-China Joint Mission on Coronavirus Disease 2019 (COVID-19) (WHO, 2020).
- [45] WHO, Pulse survey on continuity of essential health services during the COVID-19 pandemic (2020).
- [46] WHO, Statement following the twenty-eighth IHR emergency committee for polio. <https://www.who.int/news/item/21-05-2021-statement-following-the-twenty-eighth-ih-er-emergency-committee-for-polio>.
- [47] World Health Organization, Coronavirus disease (COVID-2019) situation reports (2020). <https://www.who.int/emergencies/diseases/novel-coronavirus-2019/situation-reports>. Accessed 15 April 2020.
- [48] World Health Organization. Global immunization news (GIN) June 2020. Immunization and COVID-19. Second pulse Poll to help understand disruptions to vaccination and how to respond.
- [49] The Worldometer (2020). COVID-19 CORONAVIRUS PANDEMIC. <https://www.worldometers.info/coronavirus/>. Accessed 15 April 2020.

Subscribe to Open (S2O)

A fair and sustainable open access model



This journal is currently published in open access under a Subscribe-to-Open model (S2O). S2O is a transformative model that aims to move subscription journals to open access. Open access is the free, immediate, online availability of research articles combined with the rights to use these articles fully in the digital environment. We are thankful to our subscribers and sponsors for making it possible to publish this journal in open access, free of charge for authors.

Please help to maintain this journal in open access!

Check that your library subscribes to the journal, or make a personal donation to the S2O programme, by contacting subscribers@edpsciences.org

More information, including a list of sponsors and a financial transparency report, available at: <https://www.edpsciences.org/en/math-s2o-programme>